

# University of Naples “Federico II”



Department of Clinical Medicine and Surgery

*PhD Program in*  
*Biomedical and Surgical Advanced Therapies*  
**XXX CYCLE**

**“Oleuropein effects on rat and human microcirculation”**

**Tutor:**

Prof. Antonio Colantuoni

**Candidate:**

Dr. Martina Di Maro

**Coordinator:**

Prof. Giovanni Di Minno

**ACADEMIC YEAR 2014-2017**

# Contents

<i>Abstract</i>	pag. 1
<b>1 INTRODUCTION</b>	pag. 4
1.1 The Mediterranean Diet	pag. 4
1.1.1. The olive oil	pag. 7
1.1.2. Oleuropein	pag. 9
1.2. The Microcirculation	pag. 12
1.2.1. The role of arterioles	pag. 14
1.2.2. The vasomotion	pag. 14
1.2.3. The myogenic intrinsic activity	pag. 17
1.2.4. Neural control mechanisms	pag. 18
1.2.5. The endothelium and its role in regulating blood flow	pag. 18
1.2.6. The study of microcirculation: from intravital microscopy to laser Doppler flowmetry	pag. 21
1.2.7. Spectral analysis of laser Doppler flowmetry	pag. 22
1.3. Obesity and microvascular dysfunction	pag. 24
1.3.1. Hyperlipidemia and microvascular dysfunction	pag. 25
<b>2 AIM</b>	pag. 26
<b>3 MATERIALS AND METHODS</b>	pag. 29
3.1. <i>In vivo</i> experimental study	pag. 29
3.1.1. Experimental groups	pag. 29
3.1.2. Administration of drugs	pag. 30
3.1.3. Animal preparation	pag. 30
3.1.4. Intravital Microscopy and Microvascular Parameter Evaluation	pag. 31
3.1.5. Western Blot Analysis	pag. 34
3.1.6. 2,3,5-tripheniltetrazolium Chloride Staining	pag. 34
3.1.7. DCFH-DA Assay	pag. 35
3.1.8. Sample size and statistical power	pag. 35
3.1.9. Statistical Analysis	pag. 35

3.2.Clinical study	pag. 37
3.2.1. Study Design	pag. 37
3.2.2.Study Protocol	pag. 39
3.2.3.Spectral analysis	pag. 40
3.2.4.Diet composition	pag. 40
3.2.5.Oleuropein supplementation	pag. 40
3.2.6.Compliance	pag. 41
3.2.7.Sample size and statistical power	pag. 41
3.2.8.Statistical analysis	pag. 41
<b>4 RESULTS</b>	pag. 42
4.1 The <i>in vivo</i> study	pag. 42
4.1.2.Sham-operated animals	pag. 42
4.1.3.Hyoperfused animals	pag. 42
4.1.4.Oleuropein effects on microcirculation	pag. 43
4.1.5.eNOS inhibition	pag. 44
4.1.6.eNOS expression	pag. 44
4.1.7.Tissue damage evaluation	pag. 44
4.1.8.ROS quantification	pag. 45
4.2.The clinical study	pag. 53
4.2.1.Nutritional status evaluation	pag. 53
4.2.2.SBF evaluation under resting conditions	pag. 54
4.2.3.SBF evaluation after three months dieting	pag. 54
4.2.4.PORH evaluation	pag. 55
<b>5 DISCUSSION AND CONCLUSIONS</b>	pag. 71
<b>6 REFERENCES</b>	pag. 76

# List of abbreviations

<b>aCSF</b>	artificial cerebrospinal fluid;
<b>b.w.</b>	body weight
<b>BCCAO</b>	bilateral common carotid artery occlusion;
<b>DCFH-DA</b>	2'-7'-dichlorofluorescein-diacetate;
<b>eNOS</b>	endothelial nitric oxide synthase;
<b>FITC</b>	fluorescein isothiocyanate bound to dextran, molecular weight 70 kDa;
<b>i.v.</b>	intravenously;
<b>I</b>	Hypoperfused group;
<b>LDPM</b>	laser Doppler perfusion monitoring;
<b>L-NIO</b>	N(5)-(1-iminoethyl)-L-ornithine;
<b>MABP</b>	mean arterial blood pressure;
<b>NA</b>	numerical aperture;
<b>NGL</b>	normalized grey levels;
<b>OL<sub>1</sub></b>	oleuropein low-dose;
<b>OL<sub>2</sub></b>	oleuropein high-dose;
<b>PCL</b>	perfused capillary length;
<b>PVDF</b>	polyvinylidene difluoride membranes;
<b>RE</b>	reperfusion;
<b>ROI</b>	regions of interest;
<b>ROS</b>	ROS, reactive oxygen species;
<b>S</b>	sham-operated;
<b>TTC staining</b>	2,3,5- triphenyltetrazolium chloride staining;
<b>v.l.</b>	venular length;
<b>HO group</b>	Hyperlipidemic obese females;
<b>OD group</b>	Hyperlipidemic obese females treated with diet;

<b>OL group</b>	Hyperlipidemic obese patients treated with diet plus oleuropein;
<b>NW group</b>	Normalweight females;
<b>BMI</b>	Body Mass Index;
<b>SBF</b>	Skin Blood Flow;
<b>PU</b>	Perfusion Units;
<b>PSD</b>	Power Spectral Density;
<b>PORH</b>	Post-occlusive reactive hyperemia;
<b>PK</b>	Maximum hyperemic peak.
<b>LDF</b>	Laser Doppler flowmetry
<b>FMD</b>	Flow-mediated dilation

# List of Tables

4.1. Variations of the main parameters in sham-operated subgroups	pag. 46
4.1.1. Variations of the main parameters in S subgroup, I group, OL <sub>2</sub> subgroup, L/OL group	pag. 47
4.2. Anthropometric measurements, body composition and metabolic parameters in NW, O and HO group under baseline conditions.	pag. 56
4.2.1. Anthropometric measurements and body composition under baseline conditions and after three months dieting in OL and OD groups.	pag. 57
4.2.2. Total cholesterol, HDL cholesterol, LDL cholesterol and triglycerides under baseline conditions (T <sub>0</sub> ) and after three months dieting (T <sub>1</sub> ) in OL and OD groups.	pag. 58
4.2.3. PORH peak; PORH total increase; time to peak; duration of hyperemia, under baseline conditions in NW, O and HO groups.	pag. 67

# List of Figures

1. The Mediterranean diet pyramid.	pag. 6
1.1. Olive oil phenolic compounds.	pag. 8
1.2. Oleuropein and oleuropein aglycone structure.	pag. 10
1.3. Oleuropein biosynthetic pathway.	pag. 11
1.4. Microvascular network.	pag. 13
1.5. Cyclic variations of hamster subcutaneous arterioles.	pag. 16
1.6. eNOS molecular structure.	pag. 19
1.7. (a) A typical laser Doppler flowmetry recorded from the volar side; (b) The spectrum of the laser Doppler blood flow signal in the six frequency intervals; (c) The wavelet transform of a 45-s time series section of the Laser-Doppler blood flow signal during SNP iontophoresis.	pag. 23
3.1. Experimental design of drug administration and measurement times.	pag. 32
3.2. Clinical study design.	pag. 37
4.1. Diameter changes in the experimental groups.	pag. 48
4.1.1. Computer-assisted images of pial microvascular network in one of hypoperfused rats and in one of oleuropein-treated rats, under baseline conditions and at RE.	pag. 49
4.1.2. Western blotting of eNOS expression and phosphorilated eNOS expression in two cerebral zones, cortex and striatum, at RE	pag. 50
4.1.3. TTC staining of coronal brain slice from a rat submitted to BCCAO and reperfusion (I group) and a rat treated with oleuropein.	pag. 51
4.1.4. Changes in DCF fluorescence intensity correlated to the intracellular ROS levels at the end of BCCAO and at RE in the different experimental groups.	pag. 52

4.2. Total cholesterol, LDL cholesterol and HDL cholesterol under baseline conditions and after three months of hypocaloric and hypolipidic diet in OD group.	pag. 59
4.2.1. Total cholesterol, LDL cholesterol and HDL cholesterol under baseline conditions and after three months of hypocaloric and hypolipidic diet in OL group.	pag. 60
4.2.2. Skin microvascular blood flow, expressed as Perfusion Units (PU), under baseline conditions in NW group, O group and HO group.	pag. 61
4.2.3. Total Power Spectral Density, expressed as $PU^2/Hz$ , under baseline conditions in NW group, O group and HO group.	pag. 62
4.2.4. Normalized power spectral density, expressed as percent, in NW, O and HO groups, under baseline conditions.	pag. 63
4.2.5. Skin microvascular blood flow, expressed as Perfusion Units (PU), under baseline conditions and after three months of hypocaloric and hypolipidic diet, in OD group and OL group.	pag. 64
4.2.6. Normalized power spectral density, expressed as percent, under baseline conditions and after three months of hypocaloric and hypolipidic diet in OD group.	pag. 65
4.2.7. Normalized power spectral density, expressed as percent, under baseline conditions and after three months of hypocaloric and hypolipidic diet in OL group.	pag. 66
4.2.8. Post-occlusive reactive hyperemia peak, expressed as perfusion units (PU), under baseline conditions and after three months of hypocaloric and hypolipidic diet in OD and OL groups.	pag. 68
4.2.9. Percent increase in post-occlusive reactive hyperemia, under baseline conditions and after three months of hypocaloric and hypolipidic diet in OD and OL groups.	pag. 69
4.2.10. Time to peak, expressed in seconds, under baseline conditions and after three months of hypocaloric and hypolipidic diet in OD and OL groups.	pag. 70

*To my family,*

*thank you for your unconditional love and support...*

# Abstract

Many epidemiological studies indicate that Mediterranean diet is a healthy eating plan useful in protecting against chronic disorders such as diabetes, cardiovascular and neurodegenerative ones [1-4]. Its health benefits are associated to the high consumption of certain food groups such as vegetables, fish, legumes, whole cereals and extra virgin olive oil (EVOO). In particular, EVOO, the main source of fat in the Mediterranean diet, has many protective effects on health because of its high content in monounsaturated fatty acids (MUFAs), as well as in polyphenolic compounds [5]. Among these, oleuropein and its derivatives, such as hydroxytyrosol, showed interesting antioxidant and anti-inflammatory properties so that they appeared useful in many metabolic and degenerative diseases including diabetes, hypertension, and Parkinson's disease [6-8].

The aim of the present study was to investigate oleuropein effects on microvascular responses.

First, we investigated the *in vivo* effects of oleuropein on rat pial microcirculation submitted to hypoperfusion-reperfusion injury. Therefore, we studied acute microvascular responses such as arteriolar vasodilation, permeability increase, leukocyte adhesion and capillary perfusion, by fluorescence microscopy. The working hypothesis was that this polyphenol may induce nitric oxide (NO) release from endothelial cells and consequently protect cerebral blood flow distribution and cerebral tissue. Rat cerebral cortical eNOS protein levels were evaluated as well as the impact of oxidative stress induced by hypoperfusion and reperfusion on brain tissue, utilizing DCFH-DA.

The second part of the study was aimed to evaluate oleuropein effects on skin microvascular blood flow oscillations of hyperlipidemic obese patients, by laser Doppler flowmetry (LDF). This is a non-invasive technique by which the rhythmic oscillations of blood flow in peripheral circulation, the so called flowmotion, can be assessed [9]. Moreover, laser Doppler signal analysis allows us to receive interesting informations about the influence of heart rate,

respiration, intrinsic myogenic activity, neurogenic factors and endothelial activities on cutaneous blood flow [10].

Therefore, hyperlipidemic obese patients were administered with a hypocaloric and hypolipidic diet plus oleuropein for three months. These data were compared with the response of hyperlipidemic obese patients administered with hypocaloric and hypolipidic diet. Under baseline conditions and at the end of the study, nutritional status and lipid profile were evaluated as well as skin blood flow oscillations and reactive hyperemia by LDF.

The results of the experimental study in rats indicate that oleuropein significantly improved *in vivo* microvascular responses after hypoperfusion-reperfusion injury. In particular, 20 mg/Kg b.w. of oleuropein induced a dilation by  $28 \pm 2\%$  of baseline ( $p < 0.01$  vs. I group) in order 3 arterioles and significantly reduced microvascular leakage (NGL:  $0.13 \pm 0.03$ ;  $p < 0.01$  vs. I group) as well as leukocyte adhesion on venular walls ( $2.0 \pm 0.5/100 \mu\text{m v.l./30 sec}$ ;  $p < 0.01$  vs. I group), at the end of reperfusion. Moreover, this polyphenol was able to preserve capillary perfusion at the end of reperfusion ( $-26.0 \pm 4.5\%$  of baseline;  $p < 0.01$  vs. I group). These responses were associated to the increased eNOS expression in cortex and in striatum of treated animals. Oleuropein was also able to reduce neuronal damage and ROS production at the end of reperfusion, compared with hypoperfused animals.

On the other hand, the results of the clinical study revealed that three months of hypocaloric and hypolipidic diet associated to oleuropein significantly improved nutritional status and lipid profile of hyperlipidemic obese patients. Total and LDL cholesterol, indeed, decreased by  $15.0 \pm 1.2$  and  $16.5 \pm 1.3\%$ , respectively, in patients treated with diet (OD group), and by  $21.3 \pm 1.5$  and  $21.2 \pm 1.4\%$ , respectively, in subjects treated with diet plus oleuropein (OL group).

Moreover, laser Doppler measurements showed an increase in skin perfusion, compared to baseline conditions and control group ( $+25.6 \pm 1.4\%$  of baseline), while the spectral analysis of skin blood flow oscillations revealed an increase in the NO-dependent and myogenic-related frequency components. Furthermore, PORH response improved in oleuropein-treated group, compared to controls.

In conclusion, oleuropein appeared able to protect rat pial microcirculation from hypoperfusion-reperfusion injury increasing nitric oxide release from endothelial cells, reducing oxidative stress and, consequently, preserving pial blood flow distribution. Interestingly, this polyphenol showed beneficial effects also in humans; three months of hypocaloric and hypolipidic diet plus oleuropein increased smooth muscle cell functions and microvascular responses in hyperlipidemic obese patients, improving tissue perfusion.

# Chapter 1

## Introduction

### 1.1. The Mediterranean Diet

The term “Mediterranean diet” is not only representative of a healthy eating plan, well appreciated for its protective effects on health, but includes all culture and traditions of Mediterranean populations about harvesting, conservation, processing, cooking of foods and, in particular, the way to consume it.

At the beginning of '50s Ancel Keys (1904-2004), an American physiologist, PhD in Biology at the University of Minnesota, USA, was interested in studying the correlation between cardiovascular disease and diet in the United States, because Americans were dying younger than peoples in many other Countries. Keys hypothesized that this phenomenon might depend on nutrition and, after interesting conversations with the Prof. Gino Bergami, physiologist at the University of Naples, left for the southern of Italy, where the myocardial infarction was not as common as in the States.

Therefore, Keys, with the collaboration of eminent scientists around the world, investigated the relationship between Nutrition, Human Physiology and Food Culture; it was the Seven Countries Study (SCS).

During the first phase of the study (1958-1983), standardized lifestyle and risk factor surveys were carried out at baseline and after 5 and 10 years of follow-up in 16 cohorts of middle-aged men from seven Countries. The second phase of the investigation (1984-1999) was characterized by the study of cardiovascular disease in elderly populations of 9 European cohorts. 50 year mortality data were collected up to 2014 and still are in 13 of the 16 cohorts.

Fatty acids, contained in foods consumed in their own homes by volunteers of the 16 cohorts, were chemically analyzed. Therefore, Ancel Keys and colleagues detected interesting associations across cultures in the SCS;

different cultures denoted differences in their diets. Moreover, corresponding differences were seen in saturated fat, serum cholesterol and coronary heart disease (CHD) incidence after 5 and 10 years of follow-up. The data indicated that high cholesterol serum levels were associated with a higher risk of mortality from cardiovascular disease in the different SCS cohorts. In addition, serum levels of cholesterol correlated with coronary heart disease, fatal after 35 years, although this association decreased with age. Adhering to a Mediterranean style diet was associated with a 39% lower coronary mortality risk. Thus, a high consumption of bread, pasta, legumes, vegetables, fruit and fats rich in unsaturated fatty acids, a moderate intake of fish and a low intake of dairy products and meat, characteristic of a Mediterranean Diet, appeared essential to prevent cardiovascular damage [11,12,14].

In 2010, therefore, UNESCO recognized the Mediterranean Diet as Intangible Cultural Heritage of Humanity, defining the Mediterranean Diet “a social practice based on the set of skills, knowledge, practices and traditions ranging from the landscape to the cuisine, which in the Mediterranean basin concern the crops, harvesting, fishing, conservation, processing, preparation and, particularly, consumption. This set, recreated within and by the communities identified in the territories of the four States Parties (Italy, Spain, Greece and Morocco), is unavoidably linked to a seasonal calendar marked by nature and religious or ritual meanings” [13].

The Mediterranean eating plan is characterized by a daily intake of whole cereals, vegetables, legumes, fruit and olive oil; a moderate intake of fish and poultry and a lower intake of dairy products, red and processed meats, as shown in Figure 1. After Keys studies, many papers investigated the association between certain food consumption and chronic diseases such as obesity, cancer and diabetes. The Greek EPIC prospective cohort study investigated the effects of individual components of Mediterranean diet on the overall mortality. The results indicated that dominant components of the Mediterranean diet score as a predictor of lower mortality were the moderate consumption of ethanol, a low consumption of meat and processed meats, the high consumption of vegetables, fruits and nuts, olive oil, and legumes. Low contributions were found for cereals, dairy products, fish and seafood [16].

Moreover, the PREDIMED (Prevención con Dieta Mediterránea) study, demonstrated that an hypocaloric Mediterranean diet, supplemented with extra-virgin olive oil resulted in an absolute risk reduction of approximately 3 major cardiovascular events per 1000 person-years and a relative risk reduction by approximately 30%, among high-risk persons who were initially free of cardiovascular disease [17]. Many other studies showed that EVOO consumption was associated with a significant reduction of cardiovascular disease and mortality in Spanish and Italian populations [18].

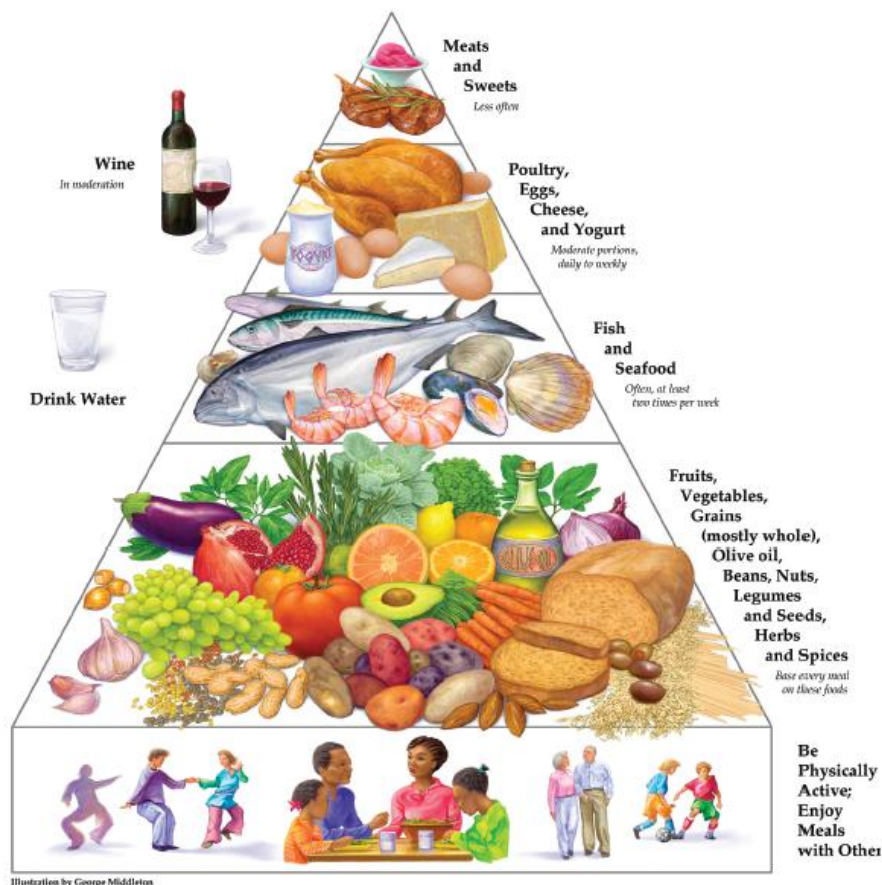


Fig.1: The Mediterranean Diet Pyramid.

### 1.1.1. The olive oil

It is well known that virgin olive oil, the main source of fat in the Mediterranean Diet, is obtained by mechanical processes from olives and can be directly consumed without any further refining treatment. Its chemical composition is characterized by two different fractions: a saponifiable and a unsaponifiable fraction [19]. The first represents the 98.5 %-99.5 % of the oil chemical composition and is constituted by triacylglycerols, diacylglycerols, monoacylglycerols, free fatty acids and phospholipids. Oleic acid (C18:1, n-9) is usually the most common monounsaturated fatty acid, even though fatty acids composition depends on different factors, such as latitude, climate and maturity of fruits. Italian, Greek and Spanish olive oils, indeed, are characterized by a high amount of oleic acid, which is around 70% of total fatty acids, while palmitic and linoleic acids are low. Previous studies showed that oleic acid was able to reduce cardiovascular risk increasing the high density lipoprotein (HDL) and reducing low density lipoprotein (LDL) levels; moreover, hypotensive effects were also demonstrated [20-22].

On the other hand, the unsaponifiable fraction contributes around 1-2 % of the oil composition and includes hydrocarbons, tocopherols, coloring pigments, sterols, phenols and triterpenes. This fraction contains many molecules with antioxidant properties, especially tocopherols and phenolic compounds. It is interesting to consider that tocopherols and carotenoids are widely diffused in nature, while phenolic substances are exclusively present in olive plants and are associated to the sensation of bitterness and pungency in oil. The mean amount of hydrophilic phenolic compounds in olive oil depends on many technological factors and can vary from 40 to 1000 mg/kg [23,24]. These molecules can be classified as phenyl acids, phenyl alcohols, flavonoids, secoiridoids and lignans (Fig.1.1).

In particular, secoiridoids, produced from the secondary metabolism of terpenes, are present only in plants of the Oleaceae family.

Secoiridoids are glycosylated compounds, characterized by the presence of elenolic acid in their structure. In particular, the most abundant secoiridoids in olives are oleuropein, demethyloleuropein, ligustroside, while nuzenide is mostly abundant in olive seeds. During olive oil production

secoiridoids undergo to hydrolysis by endogenous glucosidases, producing aglyconic corresponding forms. Therefore, the most abundant secoiridoids in olive oil are the dialdehyde form of elenolic acid linked to hydroxytyrosol (3,4-DHPEA-EDA) or tyrosol (*p*-HPEA-EDA) [25-30].

<b>Phenolic compounds</b>	
<b>Simple phenols</b>	<b>Lignans</b>
Hydroxytyrosol	(+)-Pinoresinol
Tyrosol	(+)-1-Acetoxypinoresinol
Vanillic acid	
<i>p</i> -Cumarinic Acid	<b>Secoiridoids</b>
Ferulic Acid	Glycosilated Oleuropein
4-Ethylphenol	Dimethyloleuropein
Tyrosyl Acetate	Oleuropein
Hydroxytyrosylacetate	Elenolic Acid
	Ligstroside
<b>Polyphenols</b>	Deacetyligstroside
Flavonoids	
Apigenin	
Luteolin	

Fig.1.1 : Olive oil phenolic compounds.

Many studies investigated the effects of polyphenols-enriched olive oil on health. Oliveras-Lopez et al. showed that extra-virgin olive oil rich in polyphenols reduces oxidative stress in mice pancreas [31], while Fernández-Castillejo et al., demonstrated that a polyphenol-rich olive oil enhance olive oil benefits, improving lipoprotein subclasses distribution and representing a complementary tool for the management of cardiovascular risk [32]. Among olive oil polyphenols, oleuropein and its derivatives showed strong antioxidant and anti-inflammatory activities [33,34].

### 1.1.2. Oleuropein

Oleuropein is an ester of 2-(3,4-dihydroxyphenyl) ethanol derived from mevalonic acid pathway (Fig. 1.2, 1.3) [35]. This polyphenolic compound is widely distributed in tissues of olive plants. Its concentration appears high in olive leafs and fruits, where represent the most abundant phenolic molecule. In particular, in young olives, oleuropein reaches concentrations around 14% of dry weight. However, during olive fruits maturation process, oleuropein amount significantly change, reaching lower concentrations in black olives. The oleuropein decline is due to the enzymatic activity of esterases, able to produce glucosylated derivatives of oleuropein, such as elenolic acid glucoside and demethyloleuropein, particularly abundant in black olives [36,37].

However, its content depends on different conditions such as cultivar, ripening stage and geographic origin. In particular, Italian and Greek cultivars contain high amount of oleuropein, compared to others [38].

Its antioxidant activity is closely related to the chemical structure, in which the functional group is an hydroxyl directly bonded to a benzene ring. In particular, it has been shown that, hydroxytyrosol (3,4-DHPEA) and secoiridoids containing this compound in their molecular structure, such as Oleuropein, have a strong antioxidant activity, more effective than vitamin E [39]. Therefore, many studies investigated the effects of this polyphenol by *in vitro* and *in vivo* models.

Visioli et al. hypothesized that the lower incidence of CHD and cancer, associated with the Mediterranean diet, could be related to oleuropein's antioxidant properties demonstrating that this molecule has a scavenger role

inhibiting neutrophils respiratory burst [39]. Moreover, he demonstrated that, during endotoxin challenge, oleuropein potentiates the macrophage-mediated response, resulting in higher NO production [40]. Coni et al. showed that a diet enriched with oleuropein was able to reduce LDL oxidation as well as plasmatic cholesterol levels in rabbits [41]. Moreover, this polyphenol protected isolated rat hearts from ischemia-reperfusion injury reducing creatine kinase production and the reduced glutathione release [42]. The anti-inflammatory properties of oleuropein are mainly related to its ability in inhibiting the biosynthesis of pro-inflammatory cytokines such as tumor necrosis factor  $\alpha$  (TNF- $\alpha$ ) and interleukin-1 beta (IL-1 $\beta$ ). [43]. Jemai et al. demonstrated that oleuropein derivatives improve lipid profile in rats lowering total LDL levels and inhibiting LDL oxidation [44].

Interestingly, Vissers et al. found that phenolic compounds from virgin olive oil, such as oleuropein, are highly bioavailable in humans reaching absorption values around 55–60%. Moreover, after oral ingestion, oleuropein appeared rapidly absorbed and the maximum plasma concentration occurs 2 h after administration [45]

However, to date, only few studies investigated oleuropein effects in humans. In particular, De Bock et al. showed that a diet enriched with olive leaf polyphenols was able to improve insulin sensitivity and pancreatic  $\beta$ -cell secretory capacity in overweight middle-aged men [46].

However, there are no data about the specific oleuropein effects on human microcirculation.

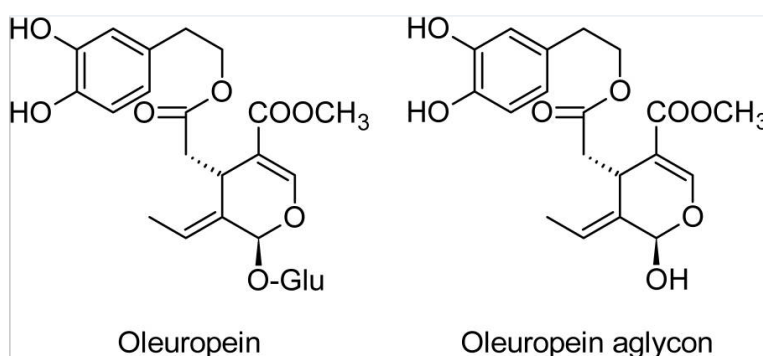


Fig.1.2: Oleuropein and oleuropein aglycone structure [47].

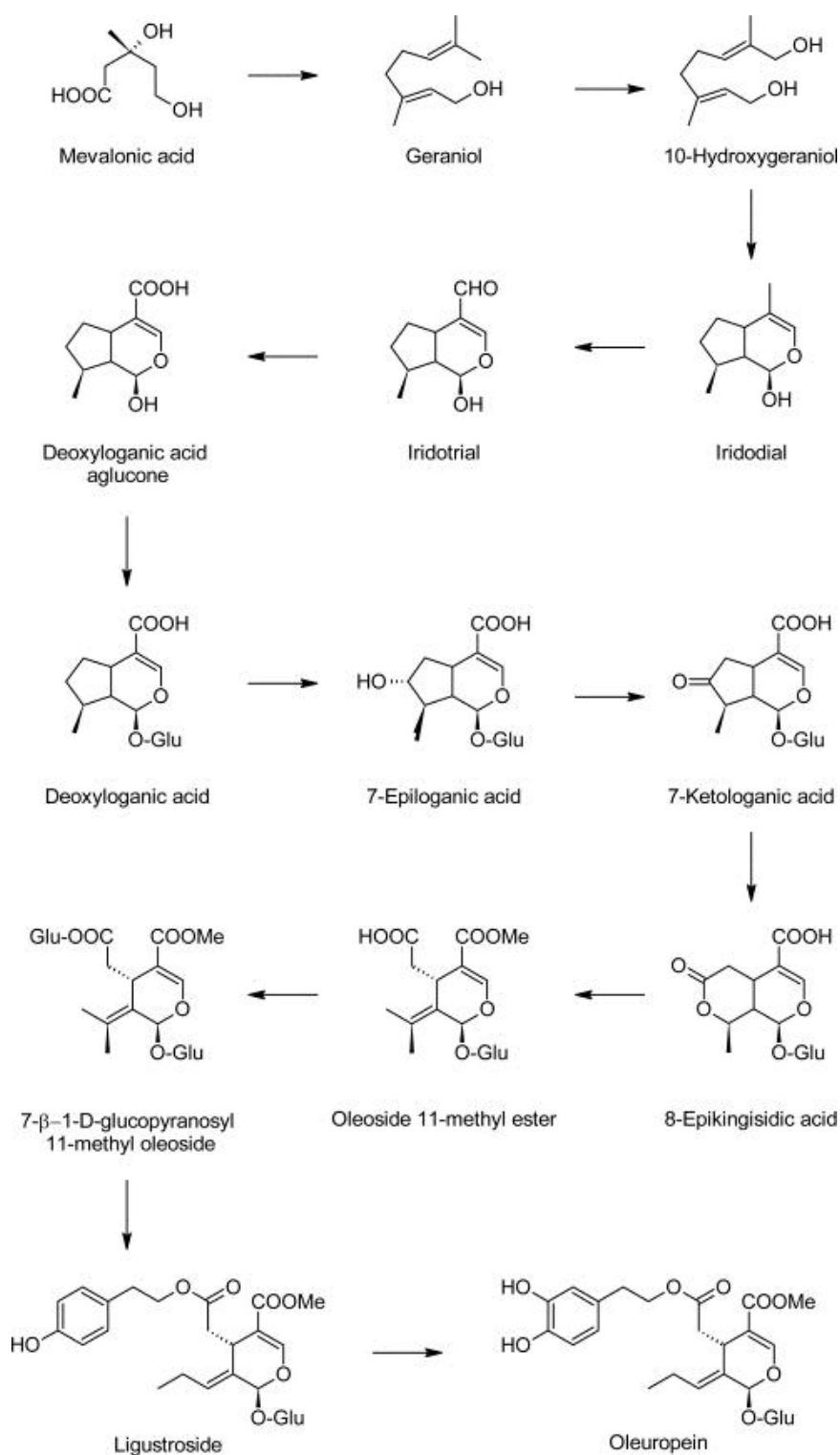


Fig.1.3: Oleuropein biosynthetic pathway [47].

## 1.2. The microcirculation

The microvascular system represents the smallest part of the circulatory system, comprising arterioles, capillaries and venules (Fig.1.4). Each portion of microvascular bed has intrinsic properties, length and cross-sectional diameter.

The arterioles are characterized by a layer of endothelial cells surrounded by the internal elastic lamina and a multilayered vascular smooth muscle and connective coat. Proceeding downstream from arterioles to capillaries, it is possible to observe localized groups of smooth muscle cells. Smaller arterioles, the so called terminal arterioles, have a mean diameter around 10  $\mu\text{m}$  and their important role is the fine regulation of blood flow. The activity of arteriole smooth muscle layer is regulated by sympathetic nerve fibers, which allow arterioles rapidly changing their tone. Moreover, gap junctions between smooth muscle cells as well as endothelial ones assure cell-cell communication and coordination of local responses.

Capillaries are the smallest vessels of microcirculation, with a diameter around 4-6  $\mu\text{m}$ . They consist of a simple endothelial layer surrounded by a basement membrane and occasional pericytes. The vessels immediately following capillaries, the so called post-capillary venules, have a mean diameter around 15-25  $\mu\text{m}$ . Vascular smooth muscle is absent in venous vessels under 30  $\mu\text{m}$ , allowing the exchange of substances between blood and interstitial fluid. The last portion of microvascular tree is characterized by collecting venules, larger vessels with contractile properties controlling the output flow [48].

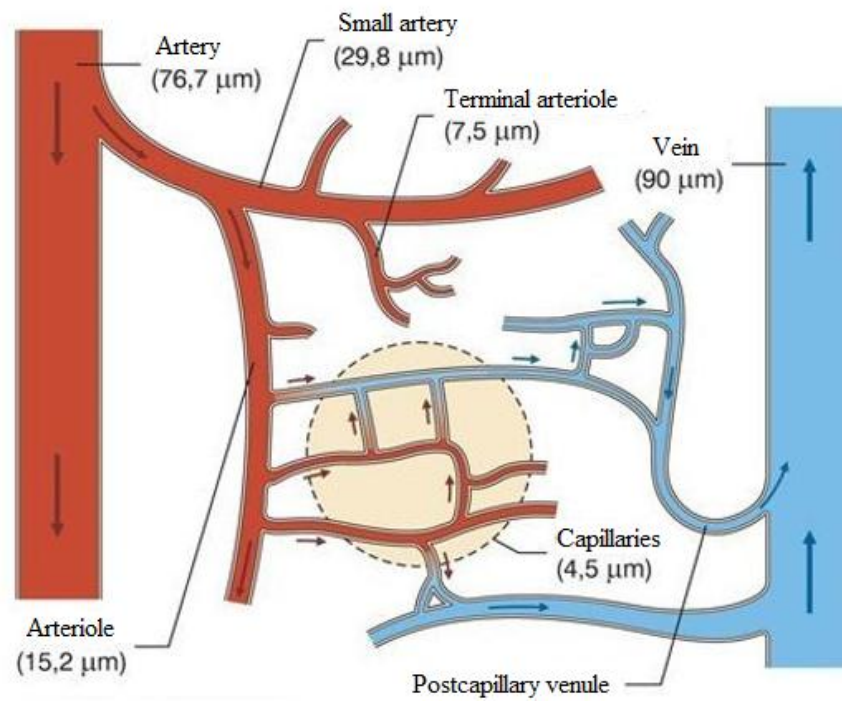


Fig. 1.4: Microvascular network [70].

### **1.2.1 The role of arterioles**

The distribution of blood flow represent a coordinated interplay between arteriolar, capillary, and venular segments according to local and regional metabolic demand. In turn, mechanisms of flow control reflect the functional interactions between skeletal muscle fibers and the respective smooth muscle cells, endothelial cells, and neural projections, which comprise and regulate the vascular supply. The regulation of muscle blood flow is presented in context of the classic Fick relationship, where the consumption of oxygen by the mitochondria within muscle fibers reflects the product of extraction from the blood and the rate of blood flow through the muscle.

Arterioles are resistance microvessels enveloped by vascular smooth muscle that by contraction or relaxation controls the vessel caliber and thus the volume of blood flow. When arterioles dilate, downstream blood flow is increased. When arterioles contract, blood flow to the downstream microvascular bed (capillaries) is reduced. Arterioles represent the most important vascular section in regulating tissue perfusion. They are able, indeed, to significantly contract and dilate, representing the primary site of vascular resistance. Their diameter, indeed, can change by up to 50% from basal levels after certain stimuli. Arterioles respond to many stimuli, such as physical ones: an elevated intravascular pressure induces arteriolar constriction, while the reduction of blood flow induces a significant arteriolar vasodilation. However, arterioles receive a variety of vasoconstrictor and vasodilator stimuli [49].

### **1.2.2. The vasomotion**

Vascular smooth muscle cells show spontaneous and rhythmic activities of contraction and relaxation; this process is called vasomotion. These oscillations of arteriolar diameter, were described for the first time by Jones in 1852 after his studies on the bat wing circulation [50]. Colantuoni et al. showed, in hamster, that the amplitude of these oscillations is strictly related to arteriolar size. In particular, smooth muscle cells of larger arterioles (with a

diameter between 50-100  $\mu\text{m}$ ) contract and dilate with a rate of 2-3 cycles per minute (cpm) with changes in diameter by 10-20 % of baseline values. In smaller vessels this oscillatory activity became faster, so that in terminal arterioles (diameter:  $<15 \mu\text{m}$ ) the frequency is around 6-12 cpm and the maximal amplitude can reach the 100% of baseline diameter [51]. Moreover, this activity does not appear synchronized throughout the microvasculature. It is well known that vasomotion is associated to slow oscillations of smooth muscle membrane potential and of intracellular  $\text{Ca}^{2+}$  concentration. Therefore, these cyclic diameter variations are induced by synchronous calcium oscillations in smooth muscle cells, achieved by gap junctions. These, indeed, allow the passage of a depolarizing current leading to the simultaneous opening of voltage-dependent  $\text{Ca}^{2+}$  channels (VDCCs) and the diffusion of calcium ions between neighboring cells. The role of gap junction in smooth muscle cells synchronization has been investigated by the use of gap junction blockers demonstrating that interruption of gap junction desynchronizes  $\text{Ca}^{2+}$  transients and membrane potential oscillations without affecting  $\text{Ca}^{2+}$  waves. Therefore, this  $\text{Ca}^{2+}$  influx, synchronized through cells, activates  $\text{Cl}^-$  and  $\text{K}^+$  conductance modulating vasomotion, as demonstrated in rat mesenteric artery [52-56]. The vasomotion can be observed only *in vitro* or *in vivo* by intravital microscopy.

Many *in vitro* and *in vivo* studies showed that endothelium activity significantly influence vasomotion because NO and cGMP have a permissive role for smooth muscle cells synchronization [57,58]. It was shown that, in isolated rat arteries, the deprivation of endothelium abolished vasomotion. Ursino et al., indeed, demonstrated that Ach decreases vasomotion frequency and increases vasomotion amplitude and arteriolar diameter, while L-NMMA causes a slight increase in vasomotion frequency and decrease in effective diameter [59]. Moreover, the endothelium-derived hyperpolarizing factor (EDHF) release is involved in this mechanism and the sympathetic nerve activity has also an important role in the regulation of vasomotion, synchronizing the activity throughout the microvascular bed [60].

Many pathological conditions affect vasomotion, such as diabetes and hypertension [85-63].

Therefore, the vasomotion is mainly due to the intrinsic myogenic activity of smooth muscle cells, but is influenced by many local and systemic regulatory mechanisms.

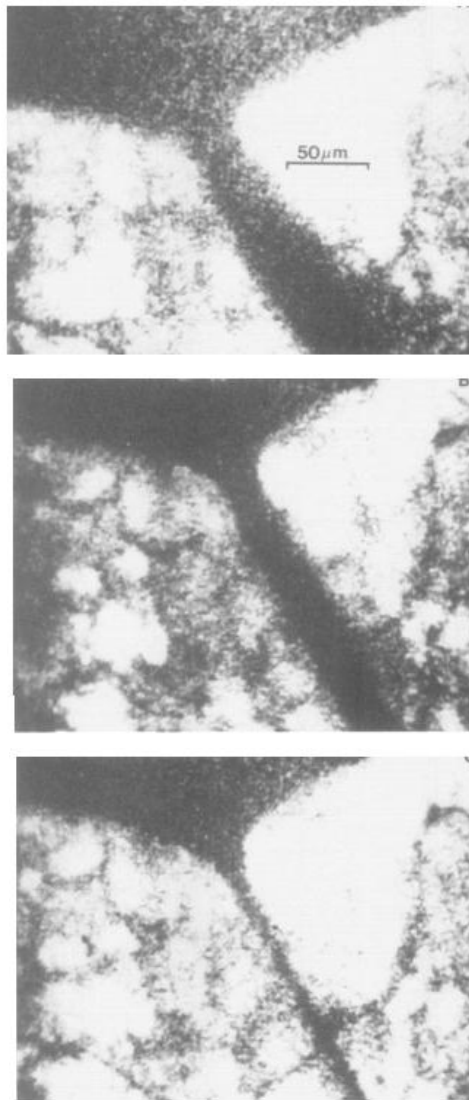


Fig. 1.5.: Cyclic variations of hamster subcutaneous arterioles; 1 sec; b) 7 sec; c) 14 sec [51].

### 1.2.3 The myogenic intrinsic activity

Smooth muscle cells are able to respond to changes in mechanical load or intravascular pressure. An elevation of transmural pressure, indeed, induces vasoconstriction, while pressure reduction induces vasodilation. The intrinsic activity of smooth muscle cells is fundamental to maintain vascular resistance, protecting smaller arterioles and capillaries from damage during perfusion changes [64]. This myogenic response is not related to endothelium or sympathetic activities, as demonstrated by many *in vitro* models.

In 1969 Uchida and Bohr showed for the first time that  $\text{Ca}^{2+}$  supply is fundamental for the maintenance of arteriolar tone [65]. Further studies demonstrated that many classes of ion channels present in vascular smooth muscle, exhibit stretch sensitivity. In particular, changes in pressure induce  $\text{Ca}^{2+}$  entry through voltage-gated  $\text{Ca}^{2+}$  channels (VGCCs) contributing to contraction through  $\text{Ca}^{2+}$ /calmodulin-induced activation of myosin light chain kinase. Therefore, gap junctions facilitate the transmission of myogenic response from the site of origin [66-69].

However, the release of vasoactive factors from endothelium and perivascular nerves as well as local metabolites can increase or decrease the level of myogenic tone and thus affect vascular resistance.

In particular, vasoactive intestinal peptide (VIP), calcitonin gene-related peptide (CGRP) and atrial natriuretic peptide (ANP) induce smooth muscle cells relaxation, while norepinephrine, noradrenaline, angiotensin II, vasopressin and neuropeptide Y (NPY) determine the contraction. Moreover, many metabolites regulate local blood flow, such as interstitial  $\text{PO}_2$ ,  $\text{PCO}_2$  and Ph, lactic acid, ATP and ADP levels. These chemical changes in interstitial fluid act directly on vascular smooth muscle cells through second messenger systems influencing the vasomotion. In particular, the reduction in  $\text{PO}_2$  or the increase in  $\text{PCO}_2$  induce, usually, vasodilation [70].

### **1.2.4 Neural control mechanisms**

The sympathetic nervous system significantly contributes to the regulation of blood flow. All arteries and arterioles, indeed, are well innervated by a complex network of noradrenergic nerve fibers producing vasoconstriction after  $\alpha_1$  receptors activation. Bigger arterioles show, usually, significant changes in diameter remaining constricted throughout the 1 min stimulation period. On the other hand, venules and veins show no response to sympathetic stimulation [71].

### **1.2.5 The endothelium and its role in regulating blood flow**

#### ***Nitric oxide.***

Nitric oxide release from endothelial cells represents one of the most important vasodilatory mechanisms regulating local blood flow. Nitric oxide (NO) diffuses from endothelial cells inducing smooth muscle cells release through the activation of soluble guanylate cyclase. This dimeric protein has two subunits containing the heme group and is able to bind NO forming a Fe-NO complex. The formation of this complex activates the enzyme, leading to GMPc accumulation. This second messenger stimulates protein kinase G (PKG) and GMPc-dependent ion channels, inducing muscle relaxation (Fig. 1.6).

Endothelial nitric oxide synthase (eNOS) is activated by several agonists, interacting with membrane receptors coupled to protein G, or by physical stimuli such as shear stress. eNOS, through basal NO production, is the key enzyme in regulating vascular tone. It is also implicated in angiogenesis, remodeling and leukocytes or platelets adhesion. Its activity is finely regulated by multiple mechanisms involving both protein-protein interactions and post-translational changes of the enzyme itself. The interaction with calmodulin is necessary for the enzymatic activity of eNOS; moreover, eNOS activity is also closely related to intracellular calcium ( $\text{Ca}^{2+}$ ) concentration [72-73].

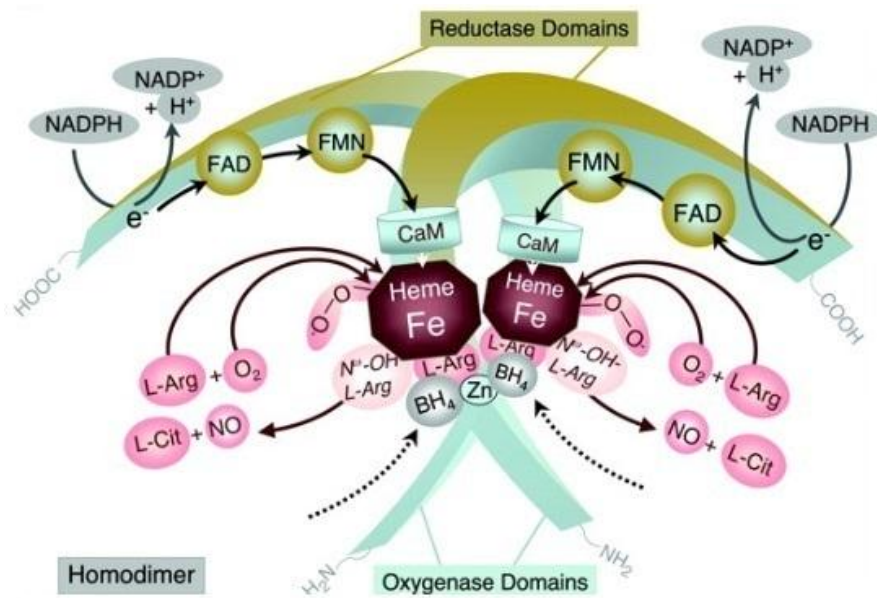


Fig.1.6.: e-NOS molecular structure [73].

***Endothelial derived hyperpolarizing factor (EDHF).***

An additional endothelium-dependent pathway inducing smooth muscle cells relaxation is called endothelium-derived.

This non-characterized endothelial factor has been associated with the hyperpolarization of the vascular smooth muscle cells by SK<sub>Ca</sub> and IK<sub>Ca</sub> channels. Their activation leads to smooth muscle cells hyperpolarization directly by gap junctions or by K efflux from the intracellular compartment toward the extracellular space.

***Prostacyclin.***

Prostacyclin is the major metabolite of arachidonic acid produced by cyclooxygenase in endothelial cells. It activates IP receptors on vascular smooth muscle and, in most physiological arteries, produces relaxation. Depending on the artery and/or the species, a hyperpolarization can occur, which involves the opening of one or more of types of potassium channels.

***Endothelins.***

Endothelial cells produce different types of endothelins, molecules with many biological effects, including vasoconstriction. The 21-amino acid peptide endothelin-1 (ET-1) is the predominant isoform of the endothelin peptide family.

ET-1 production is activated by different acute and chronic diseases such as hypertension, atherosclerosis and heart failure.

***Tromboxane A<sub>2</sub>.***

Tromboxane A<sub>2</sub> is produced by arachidonic acid metabolism. Its activation in endothelial cells increases superoxide anion radical O<sub>2</sub> levels inducing a significant reduction of NO bioavailability [71].

### **1.2.6 The study of microcirculation: from intravital microscopy to laser Doppler flowmetry.**

The study of vasomotion is possible only *in vivo* by intravital microscopy [74]. In particular, the creation of a cranial window to study the pial microcirculation represents a widely used experimental technique. The first approach, described in larger animals by Forbes in 1928, was based on an open skull window technique [75]; subsequently, Rosenblum, Zweifach and Wahl were able to observe pial microcirculation in mouse and rat [76-77]. However, the open window preparation presented many disadvantages, including the alteration of cerebrospinal fluid composition and the risk of brain herniation, especially during conditions such as hypoxia; all these factors significantly affected the microvascular analysis [78]. Therefore, in 1986, Morii et al. developed a closed cranial window technique to study the reactivity of rat pial arterioles and venules to adenosine and carbon dioxide. This approach is now still used; the window (4 mm x 5 mm) is usually implanted above the left frontoparietal cortex so that the skull is exposed and the craniotomy is performed to remove the dura mater and to put in position a quartz microscope coverglass [79]. By fluorescent tracers, intravenously injected, it is possible to visualize vessels and characterize arteriolar tree, according to diameter, length and branchings. Lapi et al., indeed, characterized the geometric distribution of rat pial vessels demonstrating that arterioles respond in a size-dependent manner to acute stimuli such as hypoperfusion-reperfusion injury [80].

On the other hand, the direct study of arteriolar diameter changes is not possible in humans. However, the study of cyclic variations of blood flow in vessels, the flowmotion, allow us to receive informations about many physiological mechanisms influencing the microcirculation, such as the activity of smooth muscle cells [81,82]. The analysis of flowmotion can be assessed by laser Doppler flowmetry (LDF), a non-invasive technique useful in evaluating blood flow distribution to tissues. Tissue perfusion, indeed, is recorded by the application of a probe emitting a low-power monochromatic laser light on the

skin. The perfusion estimated by this technique is based on the assessment of the Doppler shift, which is scattered by moving red blood cells. The frequency and amplitude of the doppler effect are directly related to the number and velocity of red blood cells, not to their direction [83]. Many studies demonstrated the relationship between LDF and fluorescence flowmetry, venous occlusion plethysmography and heat thermal clearance [84]. Moreover, clinical applications of LDF have been previously demonstrated [85-89].

### **1.2.7 Spectral analysis of laser Doppler Flowmetry**

The oscillations of microvascular blood flow can be divided into different components by spectral analysis [90]. The Wavelet analysis proposed by Morlet (1983) is a scale-independent method comprising an adjustable window length [91]. Stefanovska et al. demonstrated that skin blood flow oscillations, recorded by laser Doppler flowmetry, can be analyzed by the Wavelet transform to receive informations about the influence of several physiological factors, involved in the regulation of blood flow: the NO-independent and NO-dependent endothelial activities, the sympathetic nervous system discharge, the intrinsic myogenic activity of vascular smooth muscle cells, the respiration and the heart rate [92, 95].

After spectral analysis of laser Doppler flowmetry, indeed, is possible to detect six characteristic frequency peaks within the interval 0.005–2 Hz. In this range, lower oscillations, between 0.005-0.0095 and 0.0095-0.21 Hz, have been related to NO independent and dependent endothelial cell activity. Moreover, the oscillations included in the range 0.021-0.052 Hz and 0.052–0.145 Hz are related with the discharge of sympathetic nervous system (neurogenic activity) and the activity of the smooth muscle cells (intrinsic myogenic activity), respectively. On the other hand, higher frequency components, included in the ranges 0.145–0.6 and 0.6–1.6 Hz, are associated to central regulatory mechanisms, such as the respiration and the heart beat, respectively (Fig.1.7.) [93-98].

Therefore, spectral analysis of LDF allow us to study the influence of local and central mechanisms regulating skin blood flow distribution.

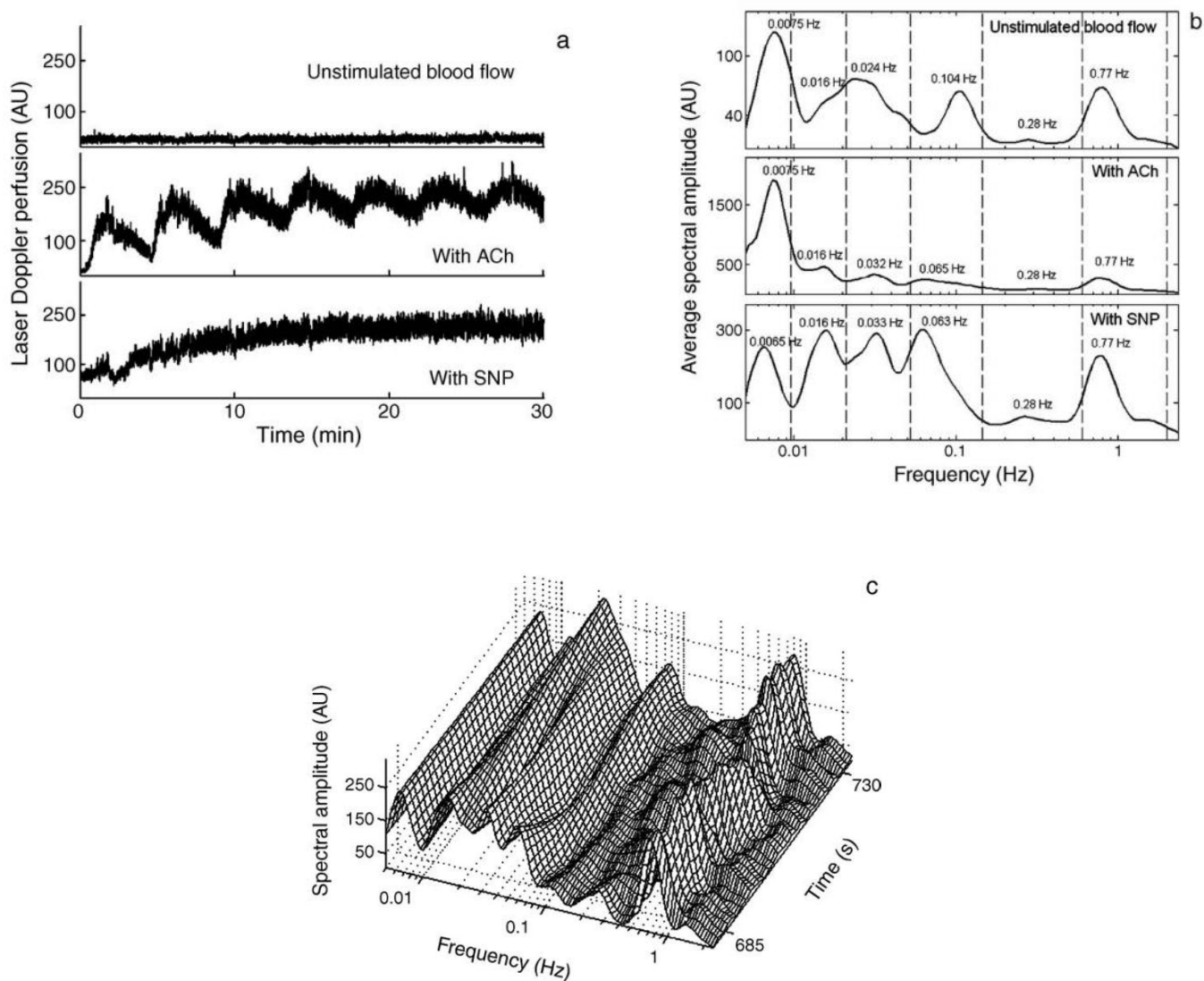


Fig. 1.7: (a) A typical laser Doppler flowmetry tracing recorded from the volar side of the forearm during unstimulated blood flow (top), during iontophoresis with acetylcholine (ACh) (middle) and sodium nitroprusside (SNP) (bottom). (b) The spectrum of the laser Doppler blood flow signal in the six frequency intervals during unstimulated blood perfusion (top), during iontophoresis with ACh (middle) and SNP (bottom). The vertical lines indicate the outer limits of each frequency interval. (c) The wavelet transform of a 45-s time series section

of the Laser-Doppler blood flow signal during SNP iontophoresis. In the three-dimensional plane the spectrum of the section is presented as the function of time and frequency and expressed in AU [95].

### **1.3 Obesity and microvascular dysfunction**

The prevalence of obesity is progressively increasing worldwide [99]. In particular, recent data indicate that 35,3% of Italian's adult population is overweight, while 9,8% is obese. The regions of the South show higher percentage of obese individuals reaching values around 39% in Campania [100].

Obesity is defined as a condition when body mass index (BMI) is greater than  $30 \text{ kg/m}^2$  and results from the interaction between genetic predisposition, wrong food habits and sedentary lifestyle. However, many studies showed that abdominal obesity represents an important predictor of metabolic and cardiovascular diseases independently of BMI. Visceral fat, indeed, is not an inert tissue, but a functional endocrine organ. It produces several cytokines, such as tumor necrosis factor- $\alpha$  (TNF- $\alpha$ ) and IL-6, inducing a chronic low-grade inflammatory state leading to the development of diabetes, hypertension and hyperlipidemia [101,102]. Abdominal fat reduction represents the first therapeutic approach in obese patients and even a moderate weight loss decreases abdominal fat and lipid content, reducing insulin resistance risk [103].

It is well known that obesity is strictly associated to structural and functional changes of microcirculation contributing to organ damages and insulin resistance [104]. In particular, arteriolar tone appears affected in obese subjects and endothelial response to vasodilator factors, such as acetylcholine, blunted. Moreover, the capillary recruitment to reactive hyperemia and shear stress appears significantly reduced [105-108]. Clerk et al. demonstrated an impaired muscle microvascular effect of insulin in obese subjects [109]. Moreover, the skeletal muscle microcirculation of obese individuals is characterized by a decreased capillary density, a phenomenon called rarefaction [110], and vascular remodeling [111].

Therefore, obesity represents the primary cause of microvascular dysfunction, resulting in changes in tissue perfusion.

### **1.3.1 Hyperlipidemia and microvascular dysfunction**

It is well known that hyperlipidemia is one of the main risk factors associated to atherosclerosis leading to the alteration of structure and function of the arterial wall, according with the inflammatory response [112]. Interestingly, many studies indicate that hyperlipidemia induces microvascular alterations long before the appearance of fatty streak lesions in large arteries. These microvascular changes have been demonstrated in animals fed a cholesterol-rich diet for two weeks [113,114]. Hyperlipidemic animals, indeed, showed a typical inflammatory phenotype in microvessels, characterized by an increased leukocytes and platelets adhesion to vessel walls and an enhanced oxygen radical production [114,115]. In particular, previous studies indicate that hypercholesterolemia reduces the ability of arteriolar endothelial cells to produce bioactive NO and directly affects vascular smooth muscle cell function increasing coronary arteriolar contractibility in response to norepinephrine [113,116,117]. All these mechanisms influence arteriolar structure and function, affecting smooth muscle tone and tissue perfusion.

Moreover, hyperlipidemia causes stasis and aggregation of erythrocytes in capillaries as well as a reduced deformability of red blood cells [118,119].

Granger demonstrated that, in experimental models, hyperlipidemia exacerbates the capillary response to ischemia-reperfusion injury significantly increasing microvascular permeability, compared to controls [120]. An enhanced expression of P-selectin, ICAM-1, and VCAM-1 is evident on venular walls of hypercholesterolemic animals, consequently inducing leukocyte rolling, adhesion and migration through vascular wall. All these mechanisms increase radical oxygen production, decreasing NO bioavailability in microvascular endothelium [121].

# Chapter 2

## Aim

Epidemiological studies clearly demonstrate that Mediterranean diet is a healthy eating plan associated with a reduction of acute and chronic diseases [1-4,16-18]. Many Authors focused the attention on the beneficial properties of extravirgin olive oil, the main source of fats in the Mediterranean Diet, because of its high amount in monounsaturated fatty acids, vitamins and polyphenols. Consequently, the effects of polyphenol rich olive oil on health have been well studied in clinical trials, demonstrating several improvement in endothelial function, inflammation levels and lipid profile [31,32].

However, the effects of oleuropein on microvascular function have not been fully clarified. *In vivo* studies have shown that this molecule is able to reduce LDL oxidation and plasma cholesterol levels in rabbits [41]. In addition, Manna et al. showed that oleuropein protects isolated rat hearts from oxidative damage induced by ischemia-reperfusion injury [42]. This polyphenol appears able to reduce VCAM-1 expression on endothelial wall, leukocyte adhesion and metalloprotease 9 expression [47]. Oleuropein's antioxidant, anti-inflammatory and antiatherogenic properties indicate that this molecule may protect microcirculation by acute damage, such as hypoperfusion-reperfusion injury. Therefore, the first aim of the present study was to evaluate the *in vivo* protective effects of oleuropein on rat pial microvascular responses induced by 30 min hypoperfusion and 60 min reperfusion. Rat pial microcirculation was visualized by fluorescence microscopy technique. The hypoperfusion was induced by transient bilateral common carotid arteries occlusion. Subsequently, after arterial occlusion removal, the microcirculation was observed for 60 minutes (reperfusion period).

We studied oleuropein effects on microvascular parameters, such as arteriolar diameter changes, microvascular permeability increase, leukocyte

adhesion to vessel walls and capillary perfusion. We chose to evaluate pial arteriolar changes because these vessels constitute a complex network characterized by at least five orders of vessels, regulating blood flow to the surrounding cerebral tissue [80].

The working hypothesis was that this polyphenol could induce vasodilation through the NO release, as previously described [122] and consequently protect cerebral blood flow distribution and cerebral tissue. Therefore, we studied the effects of inhibiting endothelial nitric oxide synthase (eNOS) by N(5)-(1-iminoethyl)-L-ornithine (L-NIO), prior to oleuropein administration, on microvascular responses. Moreover, rat cerebral cortical and striatum eNOS protein levels were evaluated; finally, oxidative stress induced by hypoperfusion and reperfusion on brain tissue was quantified utilizing 2'-7'-dichlorofluorescein-diacetate test (DCFH-DA).

The second part of the study was focused on the oleuropein effects on skin blood flow oscillations of hyperlipidemic obese females administered with a hypocaloric and hypolipidic diet. We hypothesized that skin microvascular function can mirror the state of microcirculation in other microvascular beds, as previously demonstrated [123,124]. Hypercholesterolemic patients, affected by coronary artery disease, are characterized by a blunted skin vasodilator response to Ach. Moreover, Rossi et al. showed that hypercholesterolemic patients without clinically manifest arterial diseases showed early sign of skin endothelial dysfunction, detected by laser Doppler flowmetry [125].

Therefore, we investigated skin microvascular blood flow impairments in newly diagnosed hyperlipidemic obese subjects using noninvasive LDF technique. Skin microvascular blood flow (SBF) was evaluated under resting conditions in all recruited patients. Moreover, to assess the peripheral microvascular reactivity, we detected the post-occlusive reactive hyperemia (PORH). Oscillations in blood flow were analyzed by spectral analysis of LDPM signals to study the influence of central and local regulatory mechanisms on skin blood flow distribution [95-97]. Finally, the effects of an oleuropein rich diet, administered for 3 months, were investigated. These data were compared with those detected in hyperlipidemic obese patients administered with hypocaloric and hypolipidic diet. Under baseline conditions,

hyperlipidemic obese subjects were compared with an age-matched group of normolipidemic obese people and an age-matched group of normal weight individuals.

# Chapter 3

## Materials and Methods

### 3.1. *In vivo* experimental study

#### 3.1.1. Experimental Groups

All experiments are conform to the Guide for the Care and Use of Laboratory Animals published by the US National Institutes of Health (NIH Publication No. 85–23, revised 1996) and to institutional rules for the care and handling of experimental animals. The protocol was approved by the “Federico II” University of Naples Ethical Committee.

Male Wistar rats, 250–300 g b.w. (Harlan, Italy), were used and randomly assigned to four groups.

1. The first group included animals not subjected to BCCAO and reperfusion [Sham Operated group, n = 14]. Five animals received 1.5 mL physiological saline solution i.v. injected (S subgroup, n = 5). Moreover, S rats received i.v. oleuropein 10 or 20 mg/kg b.w. (S/OL<sub>1</sub> and S/OL<sub>2</sub> subgroups; n = 3, respectively) or i.v. L-NIO 10 mg/kg b.w. (S/L subgroup, n = 3).
2. Hypoperfused rats (I group, n = 19) were treated with 1.5 mL vehicle i.v. injected (physiological saline solution) and subjected to 30 minutes of BCCAO and 60 minutes of reperfusion.
3. OL group (OL<sub>1</sub> subgroup, n = 5; OL<sub>2</sub> subgroup, n = 19) was administered with i.v. oleuropein, 10 or 20 mg/kg b.w., respectively, 10 minutes prior to BCCAO and at the beginning of reperfusion.
4. The fourth group of animals (L/OL group, n = 19) was administered with i.v. L-NIO (10 mg/kg b.w.) prior to i.v. oleuropein (20 mg/kg b.w.), 10 minutes before BCCAO and at the beginning of reperfusion.

For all groups, five animals were used for microvascular observations; five animals were utilized to evaluate the eNOS expression by western blotting.

Three animals were used to determine neuronal damage by 2,3,5-triphenyltetrazolium chloride staining and six animals were submitted to DCFH-DA assay after I (n = 3) or after reperfusion (n = 3). Animals belonging to OL<sub>1</sub> subgroup were exclusively utilized for microvascular studies.

### **3.1.2. Administration of Drugs**

Oleuropein solution was obtained dissolving 10 or 20 mg/kg b.w. in 0.5 mL saline solution and i.v. infused (three minutes) into the rats 10 minutes before BCCAO and at the beginning of reperfusion, as previously described [122]. L-NIO (10 mg/kg b.w) was dissolved in 0.5 mL saline solution and i.v. administered prior to oleuropein (20 mg/kg b.w.) according to the protocol time schedule reported in Figure 3.1. In preliminary experiments L-NIO infusion at the dosage of 10 mg/kg b.w. chosen for the present study, abolished vasodilation due to topical application of acetylcholine, 100  $\mu$ M (n = 10), where the diameter increase was by  $23.8 \pm 2.5\%$  of baseline under control conditions (n = 10). DCFH-DA was mixed with aCSF to obtain a concentration of 250 mM [129]. This solution was superfused over the pial surface for 15 minutes during BCCAO or reperfusion. The drugs were purchased from Sigma Chemical, St. Louis, MO, USA.

### **3.1.3. Animal Preparation**

Anesthesia was induced with a-chloralose (50 mg/kg b.w. intraperitoneal injection) and maintained with 30 mg/kg/h intraperitoneal injection. Rats were tracheotomized, paralyzed with tubocurarine chloride (1 mg/kg/h, i.v.), and mechanically ventilated with room air and supplemental oxygen. The right and left common carotid arteries were isolated for successive clamping. A catheter was placed in the left femoral artery for arterial blood pressure recording and blood gases sampling. Another one in the right femoral vein for injection of the fluorescent tracers and drugs. FITC, 50 mg/100 g b.w., i.v. as 5% wt/vol solution in three minutes administered just once at the beginning of experiment after 30 minutes of the preparation stabilization;

rhodamine 6G, 1 mg/100 g b.w. in 0.3 mL, as a bolus with supplemental injection throughout BCCAO and reperfusion (final volume 0.3 mL/100 g/h) to label leukocytes for adhesion evaluation, were the tracers. Blood gas measurements were carried out on arterial blood samples withdrawn from arterial catheter at 30 minutes time period intervals (ABL5; Radiometer, Copenhagen, Denmark). Throughout all experiments, MABP, heart rate, respiratory CO<sub>2</sub>, and blood gases values were recorded and maintained stable within physiological ranges. Rectal temperature was monitored and preserved at 37.0±0.5°C with a heating stereotaxic frame where the rats were secured. To observe the pial microcirculation, a closed cranial window (4 mm x 5 mm) was implanted above the left frontoparietal cortex (posterior 1.5 mm to bregma; lateral, 3 mm to the midline), as previously reported [126]. Briefly, the dura mater was gently removed and a 150-µm-thick quartz microscope cover glass was sealed to the bone with dental cement. The window inflow and outflow were assured by two needles secured in the dental cement of the windows so that the brain parenchyma was continuously superfused with aCSF [79,127]. The rate of superfusion was 0.5 mL/min controlled by a peristaltic pump. During superfusion the intracranial pressure was maintained at 5±1 mmHg and measured by a Pressure Transducer connected to a computer. The composition of the aCSF was: 119.0 mM NaCl, 2.5 mM KCl, 1.3 mM MgSO<sub>4</sub>, 1.0 mM NaH<sub>2</sub>PO<sub>4</sub>, 26.2 mM NaHCO<sub>3</sub>, 2.5 mM CaCl<sub>2</sub>, and 11.0 mM glucose (equilibrated with 10.0% O<sub>2</sub>, 6.0% CO<sub>2</sub>, and 84.0% N<sub>2</sub>; pH 7.38 ± 0.02). The temperature was maintained at 37.0 ± 0.5°C. The reduction of cerebral blood flow was produced by the placement of two atraumatic microvascular clips for 30 minutes on common carotid arteries, previously isolated. After removing the clamp, the pial microcirculation was observed for 60 minutes (reperfusion period).

### **3.1.4. Intravital Microscopy and Microvascular Parameter Evaluation**

Observations of pial vessels were conducted by a fluorescence microscope (Leitz Orthoplan, Wetzlar, Germany) fitted with long-distance

objectives [2.5X, NA 0.08; 10X, NA 0.20; 20X, NA 0.25; 32X, NA 0.40], a 10 X eye piece and a filter block (Ploemopak; Leitz) as previously described [126]. Epiillumination was provided by a 100 W mercury lamp using the appropriate filters for FITC, for rhodamine 6G, and a heat filter (Leitz KG1). The pial microcirculation was televised with a DAGE MTI 300RC low-light level digital camera and recorded by a computer-based frame grabber (Pinnacle DC10 plus; Avid Technology, Burlington, MA, USA). Microvascular measurements were made off-line using a computer-assisted imaging software system (MIP Image, CNR, Institute of Clinical Physiology, Pisa, Italy). The visualization of pial microcirculation was carried out according to the protocol time schedule reported in Figure 3.1.

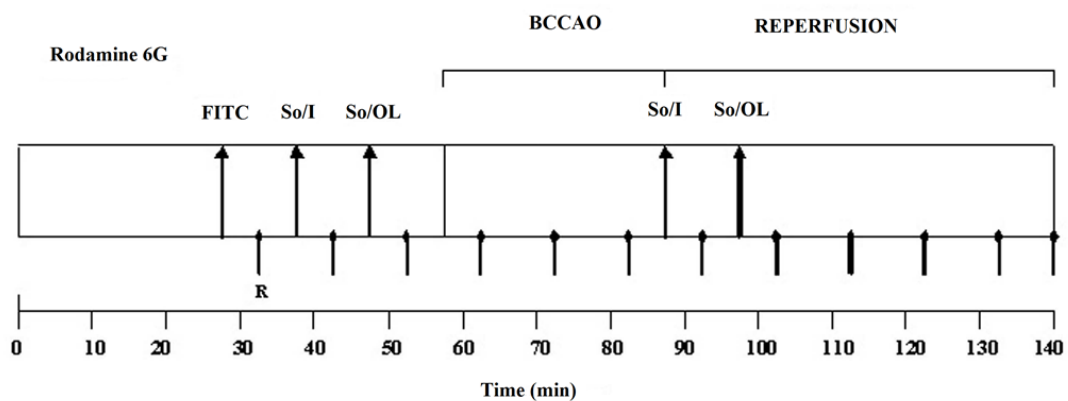


Fig.3.1.: Experimental design of drug administration and measurement times. R: recording points. FITC: fluorescent-dextran (70kDa) and rhodamine 6G. So/I: solvent, 0.9% NaCl, and/or inhibitor administration (L-NIO). So/OL: solvent, 0.9% NaCl, and/or oleuropein administration. BCCAO: bilateral common carotid artery occlusion. Rhodamine 6G was injected after FITC dextran as a bolus and then infused during BCCAO and reperfusion.

Briefly, recording of microvascular images was performed for one minute every five minutes during substance administration, before BCCAO and at the beginning of reperfusion. Afterward, recording was carried out every 10 minutes during BCCAO and the remaining reperfusion. The baseline conditions were represented by microvascular values detected within two minutes of FITC administration. The pial arteriole responses to the different substances were homogeneous during BCCAO and reperfusion; therefore, we chose to present data recorded under the baseline conditions, at the end of BCCAO and RE. Under baseline conditions, the arteriolar network was mapped by stop-frame images and pial arterioles were classified according to a centripetal ordering scheme (Strahler's method, modified according to diameter), as previously described [126]. In each animal, one order 4, two order 3 and two order 2 arterioles were studied during each experiment. Because of the homogeneous responses, we chose to present only the data regarding order 3 vessels. Arteriolar diameters were measured with a computer-assisted method (MIP Image program, frame by frame). The results of diameter measurements were in accord with those obtained by shearing method ( $\pm 0.5 \mu\text{m}$ ). To avoid bias due to single operator measurements, two independent "blinded" operators measured the vessel diameters. Their measurements overlapped in all cases. The increase in leakage was calculated and reported as NGL:  $\text{NGL} = (I - I_r)/I_r$ , where  $I_r$  is the average baseline grey level at the end of vessel filling with fluorescence (average of five windows located outside the blood vessels with the same windows being used throughout the experimental procedure), and  $I$  is the same parameter at the end of BCCAO or RE. Grey levels ranging from 0 to 255 were determined by the MIP Image program in five ROI measuring  $50 \mu\text{m} \times 50 \mu\text{m}$  (10x objective). The same location of ROI during recordings along the microvascular networks was provided by a computer-assisted device for XY movement of the microscope table. Adherent leukocytes (i.e., cells on vessel walls that did not move over a 30-second observation period) were quantified in terms of number/ $100 \mu\text{m}$  of v.l./30 sec using higher magnification (20x and 32x, microscope objectives). In each experimental group 45 venules were studied. PCL was measured by MIP image in an area of  $150 \mu\text{m} \times 150 \mu\text{m}$ . In this system, the length of perfused capillaries is easily established by the automated

process because it is outlined by dextran. MABP (Viggo-Spectramed P10E2 transducer, Oxnard, CA, USA – connected to a catheter in the femoral artery) and heart rate were monitored with a Gould Windograf recorder (model 13-6615-10S, Gould, OH, USA), connected to a computer. Blood gas measurements were carried out on arterial blood samples with drawn from arterial catheter at 30 minutes time period intervals (ABL5; Radiometer, Copenhagen, Denmark). The hematocrit was measured under baseline conditions, at the end of BCCAO and at RE. Furthermore, microvascular blood flow was measured by LDPM on the skull of all animals using a Perimed PF5000 flowmeter with a probe (457; Perimed, Jarfalla, Sweden) attached to the bone. The sampling rate was 32 Hz and blood flow was expressed as PU. We chose to present only LDPM blood flow data of hypoperfused rats (I group) and oleuropein-treated animals (OL<sub>2</sub> subgroup), to simplify data presentation.

### **3.1.5. Western Blot Analysis**

Protein concentrations were determined by the Bio-Rad protein assay (Bio-Rad, Berkeley, CA, USA). Equal amounts of proteins were separated by SDS-PAGE under reducing conditions and then transferred to (PVDF; Invitrogen, Carlsbad, CA, USA). The immunoblot was blocked, incubated with specific antibodies at 4°C overnight, washed, and then incubated for one hour with horseradish peroxidase-conjugated secondary antibody (1:2000) (GE-Healthcare, Little Chalfont, UK). Peroxidase activity was detected by enhanced chemiluminescence system (GE-Healthcare). The optical density of the bands was determined by the ChemiDoc Imaging System (Bio-Rad) and normalized to the optical density of  $\alpha$ -Tubulin (1:5000). To detect the proteins of interest, specific antibodies were used: rabbit polyclonal anti-eNOS (1:500) and rabbit poly-clonal anti-phosphorylated eNOS (Ser1177) (1:200). Antibodies were purchased from Santa Cruz Biotechnology, SantaCruz, CA, USA.

### **3.1.6. 2, 3, 5-triphenyltetrazolium Chloride Staining**

Rats were sacrificed after 30 minutes BCCAO and 60 minutes reperfusion. Tissue damage was evaluated by 2,3,5- TTC staining. The brains

were cut into 1 mm coronal slices with a vibratome (Campden Instrument, 752 M). Sections were incubated in 2% TTC for 20 minutes at 37°C and in 10% formalin overnight. The necrotic area site and extent in each section were evaluated by image analysis software (Image-ProPlus, Rockville, MD, USA) [128].

### **3.1.7. DCFH-DA Assay**

A CSF containing 250 mM DCFH-DA at  $37.0 \pm 0.5^\circ\text{C}$  was superfused over the pial surface. The lipophilic DCFH-DA is a stable non fluorescent probe with a high cellular permeability. DCFH-DA reacts with intracellular radicals to be converted to its fluorescent product (DCF). The remaining extracellular DCFH-DA was washed out with aCSF. The intensity of DCF fluorescence is proportional to the intra-cellular ROS level. The fluorescence intensity was determined by the use of an appropriate filter (522 nm) and estimated by NGL, with the baseline represented by pial surface just superfused by DCFH-DA [129].

### **3.1.8. Sample size and statistical power**

The sample size calculation was performed using MedCalc. The outcome for the calculation of sample size was the permeability increase at the end of reperfusion. A difference of 20% between hypoperfused and oleuropein-treated group was estimated. Power and significance levels were set at 0.80 and 0.05, respectively. Moreover, we considered a 25% of possible intraoperative death. Using these parameters we evaluated a sample size of 5 animals per group, for microvascular studies.

### **3.1.9. Statistical Analysis**

All reported values are mean  $\pm$  SEM. Data were tested for normal distribution with the Kolmogorov–Smirnov test. Parametric (Student's t tests, ANOVA, and Bonferroni post hoc test) or nonparametric tests (Wilcoxon,

Mann–Whitney, and Kruskal–Wallis tests) were used. Nonparametric tests were applied to compare diameter and length data among experimental groups. Due to the small sample size of DCFH-DA treated rats we used nonparametric tests to compare the results obtained in these animals. The statistical analysis was carried out by SPSS 14.0 statistical package. Statistical significance was set at  $p < 0.05$ .

## 3.2. Clinical study

### 3.2.1. Study design

The study protocol was approved by the Ethical Committee of the Federico II University Medical School of Naples and all patients gave written informed consent.

Under baseline conditions, forty hyperlipidemic obese subjects (HO group) were recruited from the Outpatient Clinic of the Department of Clinical Medicine and Surgery, “Federico II” University of Naples and compared with an age-matched group of normolipidemic obese people (O group) and an age-matched group of normal weight individuals (NW group). After baseline evaluations, hyperlipidemic patients were randomized in two subgroups: OL subgroup was administered with a hypocaloric and hypolipidic diet plus oleuropein (90 mg/day), while OD subgroup was treated with the hypocaloric and hypolipidic diet; the treatment lasted 12 weeks (Fig.3.2).

All patients were 55–64 years old sedentary women; those belonging to HO, divided in two subgroups, OD and OL, were hyperlipidemic and obese [body mass index (BMI)  $\geq 30$  Kg/m<sup>2</sup>; total cholesterol  $> 200$  mg/dL, LDL cholesterol  $> 130$  mg/dL, triglycerides  $> 150$  mg/dL]. Patients belonging to O group were normolipidemic obese (BMI  $\geq 30$  Kg/m<sup>2</sup>) while those of NW group were normalweight (BMI between 19 – 25 Kg/m<sup>2</sup>).

Exclusion criteria were: presence of diseases influencing body composition (cancer, osteoporosis and muscular dystrophia), heart failure and microangiopathy; weight loss medications (sibutramine, orlistat, rimonabant) and history of bariatric surgery; subjects on hormonal therapies (oestrogens, thyroxine, progesteron), anti-hypertensive therapies (Ca<sup>++</sup> channel blockers, ACE inhibitors), statins and any other antidyslipidemic agent or psychiatric drugs ; treatment with drugs influencing microvascular blood flow (such as vasodilators and anti-inflammatory drugs) and smokers.

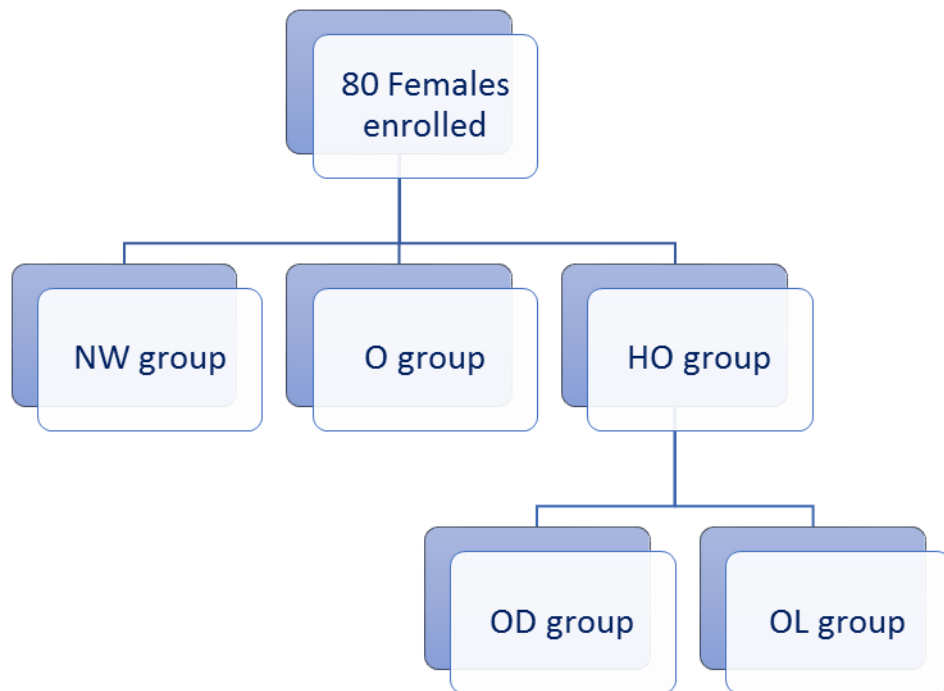


Fig.3.2.: Clinical study design. NW= normal weight group; O= obese group; HO= hyperlipidemic obese group; OD= hyperlipidemic obese females administered with hypocaloric and hypolipidic diet; OL= hyperlipidemic obese females administered with hypocaloric and hypolipidic diet plus oleuropein.

### 3.2.2. Study Protocol

Under baseline conditions and after three months of hypocaloric and hypolipidic diet, nutritional status, skin microvascular blood flow, microvascular blood flow oscillations and hyperemic response were investigated in all hyperlipidemic patients.

In particular, nutritional status was evaluated by anthropometric measurements, such as weight, height, body mass index (BMI), waist circumference (WC), hip circumference (HC) and triceps skinfold (TS). Bioimpedance analysis (Akern RJL, BIA 101) was carried out to evaluate the hydration as well as the Fat Mass (FM). Total serum cholesterol, HDL cholesterol, LDL cholesterol, triglycerides, GOT and GPT were measured.

Microvascular blood flow evaluation was performed on patients in supine position in a quiet and temperature-controlled room ( $22 \pm 3$  °C). No subjects had any medication, food, alcohol and/or drinks containing caffeine 12 h prior to the blood flow measurement. SBF was recorded using a laser Doppler perfusion monitoring apparatus (PeriFlux 5001 System, Perimed, Stockholm, Sweden). The laser Doppler probe (PF 457, Perimed, Stockholm, Sweden), connected to a computer, was placed on the right forearm volar surface. After 10 min of acclimatization, the blood flow was recorded for 20 min by a Perisoft software. The mean skin blood perfusion was expressed as arbitrary perfusion units (PU), while the power spectral density (PSD) of laser Doppler signals was reported as  $\text{PU}^2/\text{Hz}$ . Finally, skin blood flow oscillations were analyzed by the Wavelet transform [95].

Post-occlusive reactive hyperemia was evaluated in all patients under baseline conditions and after three months treatment. The brachial artery was occluded by a blood pressure cuff, placed at the right upper arm and inflated up to 50 mmHg above the systolic blood pressure. The blood pressure cuff was suddenly deflated after 3 min brachial artery occlusion. The peak value (PK), expressed as PU, was determined calculating the maximal perfusion value reached during reactive hyperemia; the percent increase in flow during hyperemic response (PK%) was calculated from the basal mean value; the time to peak ( $T_p$ ) was measured in seconds as the time from cuff release to the

maximum peak value; the duration of hyperemia was evaluated in seconds as the time from cuff release up to the recovery of the mean value.

### **3.2.3. Spectral analysis**

Microvascular blood flow oscillations, in the range 0.005 to 2.0 Hz, were evaluated by the Wavelet transform, a scale dependent method comprising an adjustable window length able to analyze both low and high frequencies. Spectral analysis was performed on 20 min recordings under resting conditions, to obtain higher resolution of very low frequency components. Wavelet analysis, proposed by Morlet, permits to detect at least six frequency components in this interval, as reported by Stefanovska et al [95]. First, the overall spectral density of each frequency interval was determined; then the normalized spectral density for each frequency interval was evaluated as the ratio between the average spectral density of a specific frequency interval and the average total power spectral density. Therefore, the relative contribution of each frequency component was defined for the entire spectrum.

### **3.2.4. Diet composition**

A Mediterranean diet, low in calories (25 kcal/kg ideal body weight) and fats, was recommended to all obese patients. The eating plan was characterized by 50-55 % of total caloric intake from carbohydrates, 15-20 % from proteins, 25% from fatty acids (< 7% saturated fats) and 30 grams of fiber per day. The daily cholesterol intake was less than 200 mg, according to the Italian guidelines suggestions [130].

### **3.2.5. Oleuropein supplementation**

Participants belonging to OL group were instructed to take one capsule/day containing 90 mg oleuropein (LongLife), orally ingested with water during dinner for three months.

### **3.2.6. Compliance**

Compliance with the dietary intervention was assessed by monitoring the dietary intake at baseline and every month until the end of the study by Food Frequency Questionnaires [131].

Assessment of compliance with the physical activity was verified by asking subjects to complete a physical activity questionnaire [132]. Compliance with the oleuropein supplementation was evaluated by the completion of a daily questionnaire asking each volunteer about the time of the consumption of the supplement as well as evaluating the presence of adverse events.

### **3.2.7. Sample size and statistical power**

The sample size calculation was performed using MedCalc. The outcome for the calculation of sample size was the increase in skin blood perfusion levels in oleuropein treated group. A difference of 20% between intervention and control was estimated. Power and significance levels were set at 0.80 and 0.05, respectively. Using these parameters the estimated sample size was of 20 participants per group.

### **3.2.8. Statistical analysis**

All data were expressed as mean  $\pm$  standard error of the mean (SEM). Data were tested for normal distribution with the Kolmogorov-Smirnov test. Parametric (Student's t tests, ANOVA and Bonferroni post hoc test) or nonparametric tests (Wilcoxon, Mann-Whitney and Kruskal-Wallis tests) were used. The statistical analysis was carried out by SPSS 14.0 statistical package. Statistical significance was set at  $p < 0.05$ .

# Chapter 4

## Results

### 4.1. The *in vivo* study

Under baseline conditions pial arterioles were classified in five orders according to diameter, length and branching, as previously described [80]. Capillaries were assigned order 0, the smallest arterioles order 1 (average diameter:  $15.7 \pm 2.0 \mu\text{m}$  and average length:  $152 \pm 74 \mu\text{m}$ ;  $n = 150$ ), while the largest ones order 5 (average diameter:  $58.5 \pm 4.2 \mu\text{m}$  and length of  $1184 \pm 330 \mu\text{m}$  ( $n = 92$ )). The values of diameters and lengths were significantly different among the different arteriolar orders ( $p < 0.01$ ) [80].

#### 4.1.2. Sham-Operated Animals

S animals did not show changes in arteriolar diameter nor increase in leakage nor adhesion of leukocytes nor decrease in capillary perfusion during the same period of observation as in the other experimental groups (Table 4.1, Figure 4.1). The S animals treated with oleuropein (at the doses of 10 or 20 mg/kg b.w.) showed a dose-related dilation of all arterioles in both subgroups. In particular, order 3 arterioles dilated by  $10 \pm 2\%$  of baseline at the higher dosage of oleuropein (S/OL<sub>2</sub> subgroup) ( $p < 0.01$  vs. baseline). We did not observe significant changes in the other parameters when compared with baseline. L-NIO did not significantly affect diameter of vessels nor the other parameters (Table 4.1).

#### 4.1.3. Hypoperfused animals

At the end of BCCAO, these animals (I group) showed a decrease in diameter of all arteriolar orders; in order 3 vessels the reduction was by 18.5

$\pm 2.0\%$  of baseline ( $p < 0.01$  vs. S subgroup and baseline) (Figure 4.1.). Microvascular leakage significantly increased compared with baseline (NGL:  $0.22 \pm 0.04$ ;  $p < 0.01$  vs. S subgroup and baseline). We did not observe changes in venular diameter, while most capillaries were not perfused (Table 4.1.1). At RE, the diameter of all arteriolar orders decreased (in order 3 by  $13.2 \pm 3.5\%$  of baseline;  $p < 0.01$  vs. S subgroup and baseline) (Figure 4.1). Microvascular leakage significantly increased (NGL:  $0.45 \pm 0.05$ ;  $p < 0.01$  vs. S subgroup and baseline) and leukocyte adhesion was markedly elevated ( $9 \pm 2/100 \mu\text{m v.l./30 sec}$ ;  $p < 0.01$  vs. S subgroup and baseline); PCL decreased by  $46 \pm 4\%$  of baseline ( $p < 0.01$  vs. S subgroup and baseline) (Table 4.1.1, Figure 4.1.1. A, B). At the end of BCCAO, microvascular blood flow recorded by LDPM on the contralateral parietal skull was reduced by  $65.0 \pm 6.5\%$  of baseline ( $p < 0.01$  vs. S subgroup and baseline,  $35.8 \pm 4.0$  PU). At reperfusion, after a transient increase ( $4 \pm 2$  minutes) in microvascular blood flow, there was a decrease of blood flow (by  $30.5 \pm 4.0\%$  of baseline;  $p < 0.01$  vs. S subgroup and baseline) up to the end of observations.

### 4.1.3 Oleuropein effects on pial microcirculation

Oleuropein (subgroups:  $OL_1$  and  $OL_2$ ) caused dose-related microvascular effects. At the end of BCCAO, the higher dose induced dilation in all arteriolar orders (by  $7.5 \pm 2.0\%$  of baseline in order 3;  $p < 0.01$  vs. I group); moreover, FD70 leakage was significantly prevented compared with hypoperfused animals (NGL:  $0.11 \pm 0.02$ ;  $p < 0.01$  vs. I group) (Table 4.1.1., Figure 4.1.). At RE all pial arterioles dilated: by  $28 \pm 2\%$  of baseline in order 3 ( $p < 0.01$  vs. I group) (Figure 4.1). Microvascular leakage was prevented (NGL:  $0.13 \pm 0.03$ ;  $p < 0.01$  vs. I group) as well as leukocyte adhesion ( $2.0 \pm 0.5/100 \mu\text{m v.l./30 sec}$ ;  $p < 0.01$  vs. I group), while capillary perfusion decreased by  $26.0 \pm 4.5\%$  of baseline ( $p < 0.01$  vs. I group) (Table 4.1.1., Figure 4.1.1. C, D). Oleuropein higher dosage increased microvascular blood flow by  $20.4 \pm 4.0\%$  of baseline ( $p < 0.01$  vs. baseline), as detected by LDPM on the contralateral parietal skull prior to BCCAO. At the end of BCCAO, there was a decrease of blood flow by  $18 \pm 7\%$  of baseline ( $p < 0.01$  vs. S

subgroup, baseline and I group). At RE blood flow increased by  $28 \pm 4\%$  of baseline ( $p < 0.01$  vs. S subgroup, baseline and I group).

#### **4.1.4 eNOS Inhibition**

At the end of BCCAO, L-NIO prior to oleuropein (group L/OL) caused reduction in diameter of all arteriolar orders: by  $5.5 \pm 1.5\%$  of baseline in order 3 ( $p < 0.01$  vs. I group and OL<sub>2</sub> subgroup) (Figure 4.1). Microvascular leakage decreased compared with hypoperfused animals ( $0.15 \pm 0.02$  NGL;  $p < 0.01$  vs. I group) (Table 4.1.1.). At RE, the diameter of all arterioles decreased (by  $6.5 \pm 2.0\%$  of baseline in order 3;  $p < 0.01$  vs. I group and OL<sub>2</sub> subgroup) (Figure 4.1). The protective effect of oleuropein on microvascular leakage was attenuated (NGL:  $0.18 \pm 0.03$ ;  $p < 0.01$ , vs. I group), leukocytes adhesion to venules was reduced ( $5 \pm 2/100 \mu\text{m v.l./30 sec}$ ;  $p < 0.01$ , vs. I group), while PCL decreased by  $32 \pm 3\%$  of baseline ( $p < 0.01$  vs. I group) (Table 4.1.1). Finally, physiological parameters, such as hematocrit, MABP, heart rate, pH, PCO<sub>2</sub> and PO<sub>2</sub> did not change in the different experimental groups up to RE (data not shown).

#### **4.1.5 eNOS Expression**

Western blot analysis revealed that eNOS protein expression increased at RE in animals treated with oleuropein compared to I and S group. In all animals the eNOS protein concentration was the higher in cortex compared to striatum. Both total and phosphorylated eNOS proteins increased to the same extent (Figure 4.1.2).

#### **4.1.6. Tissue Damage Evaluation**

The neuroprotective effects of oleuropein were assessed by evaluating damaged area after 30 minutes BCCAO and 60 minutes reperfusion. In hypoperfused rats, TTC staining revealed a massive lesion of striatum in both hemispheres, while cortical and sub-cortical areas presented slight injury. The

higher dose of oleuropein were able to reduce neuronal damage, compared with that observed in hypoperfused animals (Fig.4.1.3).

#### **4.1.7 ROS Quantification**

DCFH-DA superfusion in sham operated rats did not cause significant increase in DCF fluorescence intensity at the end of observations ( $0.04 \pm 0.02$  NGL). In hypoperfused animals DCFH-DA superfusion induced an increase in DCF fluorescence intensity at the end of BCCAO ( $0.23 \pm 0.02$  NGL,  $p < 0.01$  vs. S subgroup and baseline). The fluorescence was higher at RE ( $0.30 \pm 0.03$  NGL,  $p < 0.01$  vs. S subgroup and baseline) likely because of further increase in ROS production. Higher dose of oleuropein decreased DCF fluorescence intensity compared with hypoperfused animals: at the end of BCCAO, NGL were  $0.09 \pm 0.02$  and  $0.08 \pm 0.01$  ( $p < 0.01$  vs. I group), respectively. At RE, NGL were  $0.15 \pm 0.03$  and  $0.13 \pm 0.02$  ( $p < 0.01$  vs. I group), respectively. Administration of L-NIO prior to oleuropein did not significantly change the effects of oleuropein on ROS formation (Fig. 4.1.4.).

<b>Sham-operated subgroups</b>	<b>Number of animals (n)</b>	<b>Microvascular leakage (NGL)</b>	<b>Leukocyte adhesion (Number of leukocyte/100µm of venular length/30s)</b>	<b>Capillary perfusion (% reduction compared to baseline)</b>
<b>S/OL<sub>1</sub></b>	3	0.04± 0.02	2.0 ± 0.4	0 ± 5
<b>S/OL<sub>2</sub></b>	3	0.02± 0.01	1.0 ± 0.5	0 ± 5
<b>S/L</b>	3	0.03± 0.01	1.0 ± 0.2	0 ± 5
<b>S</b>	5	0.04± 0.02	2.0 ± 0.3	0 ± 5

Table 4.1.: Variations of the main parameters in sham-operated subgroups: S/OL<sub>1</sub> (oleuropein, 10 mg/kg b.w), S/OL<sub>2</sub> (oleuropein, 20 mg/kg b.w.), S/L (L-NIO, 10 mg/kg b.w.), S (physiological saline solution, 1.5 mL).

<b>Groups</b>	<b>Number of animals (n)</b>	<b>Microvascular leakage (NGL)</b>	<b>Leukocyte adhesion (Number of leukocyte/100µm of venular length/30s)</b>	<b>Capillary perfusion (% reduction compared to baseline)</b>
<b>S</b>	5	0.04± 0.02	2.0 ± 0.3	0 ± 5
<b>I</b>	19	0.45 ± 0.05 <sup>°</sup>	9 ± 2 <sup>°</sup>	46 ± 4 <sup>°</sup>
<b>OL<sub>2</sub></b>	19	0.13 ± 0.03 <sup>°*</sup>	2.0 ± 0.5 <sup>°*</sup>	26.0 ± 4.5 <sup>°*</sup>
<b>L/OL</b>	19	0.18 ± 0.03 <sup>°*</sup>	5 ± 2 <sup>°*</sup>	32 ± 3 <sup>°*</sup>

Table 4.1.1.: Variations of the main parameters in sham-operated (S) subgroup, hypoperfused (I) group, oleuropein (OL<sub>2</sub>) subgroup (20 mg/kg b.w.); L-NIO (10 mg/kg b.w) and oleuropein (20 mg/kg b.w.) (L/OL) group;

<sup>°</sup>p<0.01 vs S group and baseline; <sup>\*</sup>p < 0.01 vs. I group,

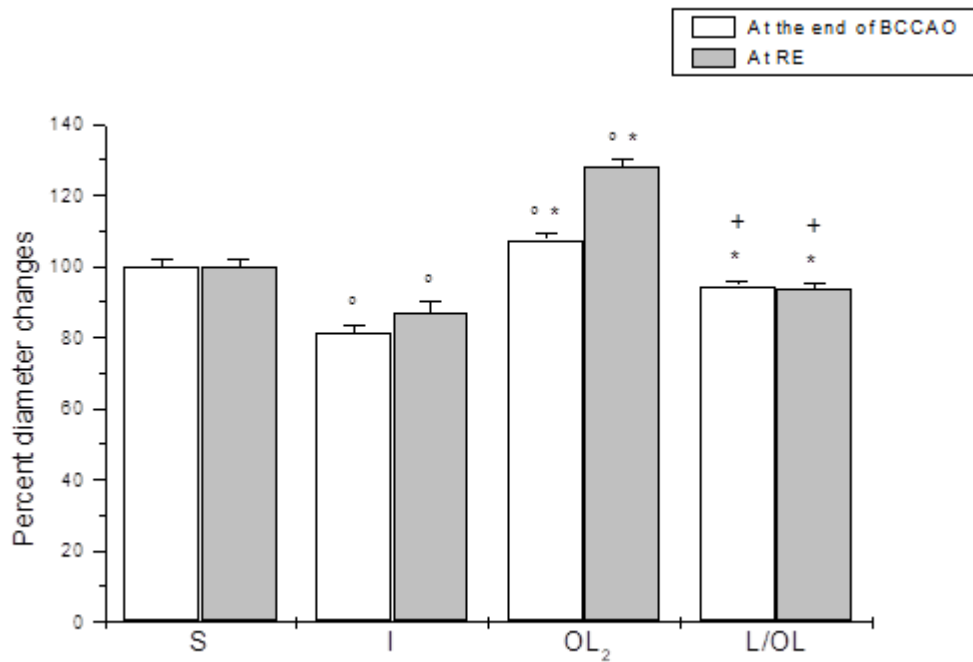


Fig. 4.1.: Diameter changes in the experimental groups. Diameter changes of order three arterioles, expressed as percent of baseline at the end of BCCAO and reperfusion (RE) in S = sham operated subgroup; I = hypoperfused group; OL<sub>2</sub> = oleuropein subgroup (20 mg/kg b.w.); L/OL = L-NIO (10 mg/kg b.w.) and oleuropein (20 mg/kg b.w.) group;

°p < 0.01 vs. S subgroup and baseline, \*p < 0.01 vs. I group, +p < 0.01 vs. OL<sub>2</sub> subgroup.

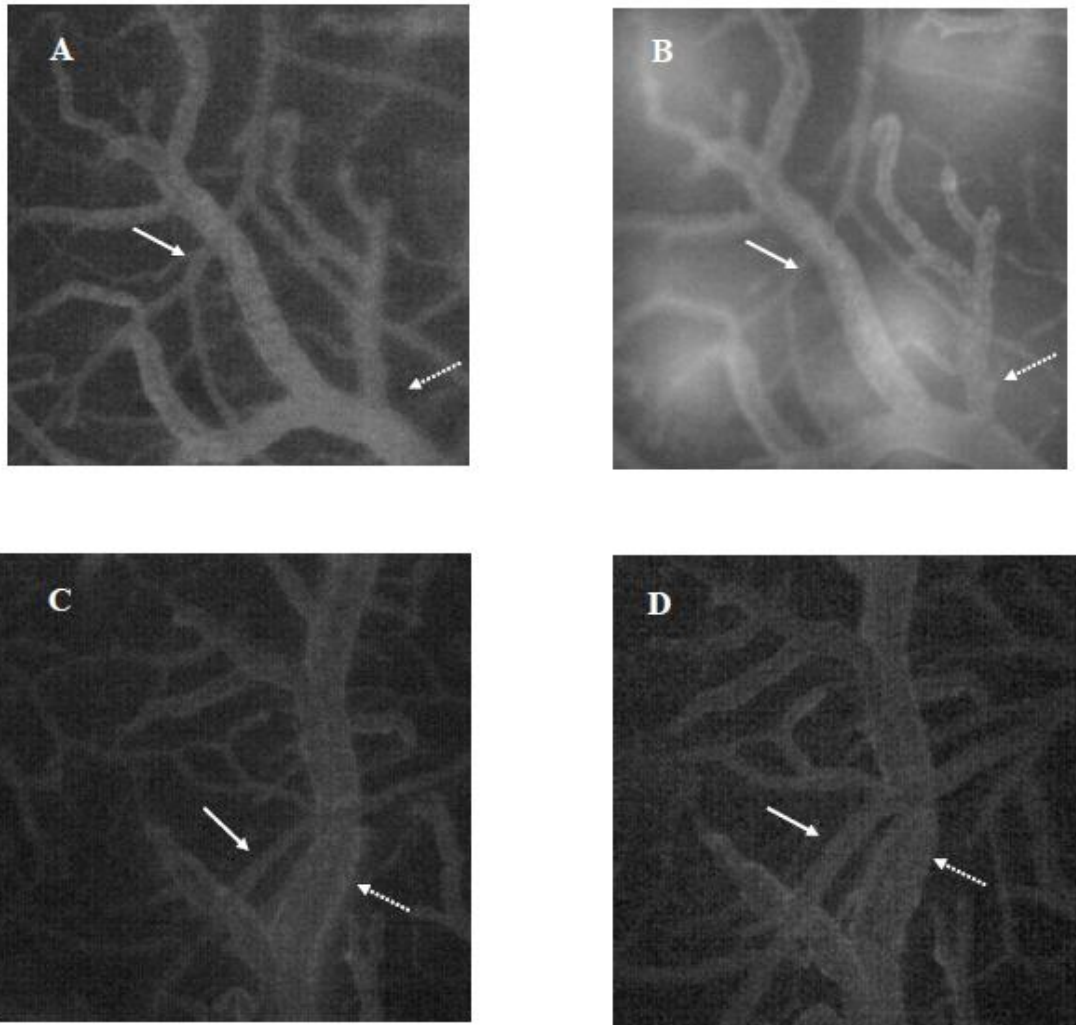
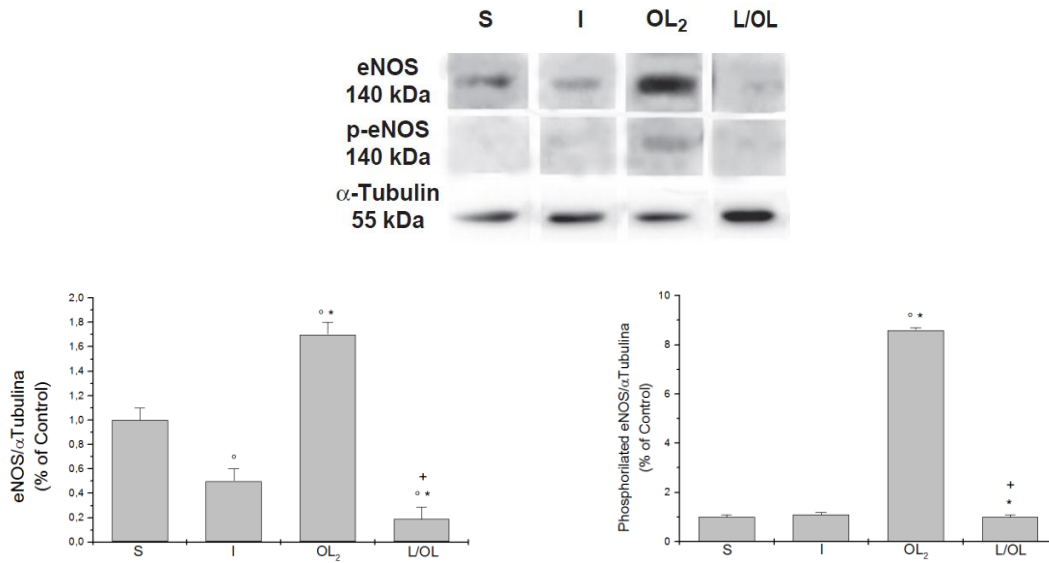


Fig.4.1.1.: Computer-assisted images of a pial microvascular network under baseline conditions (A) and RE (B) in one of the hypoperfused rats. The increase in microvascular leakage is outlined by the marked change in the color of interstitium (from black to white). Computer-assisted images of a pial microvascular network under baseline conditions (C) and RE in an oleuropein-treated rat (20 mg/kg b.w.) (D);

Scale bar = \_\_\_\_\_ 100  $\mu$ m.

## CORTEX



## STRIATUM

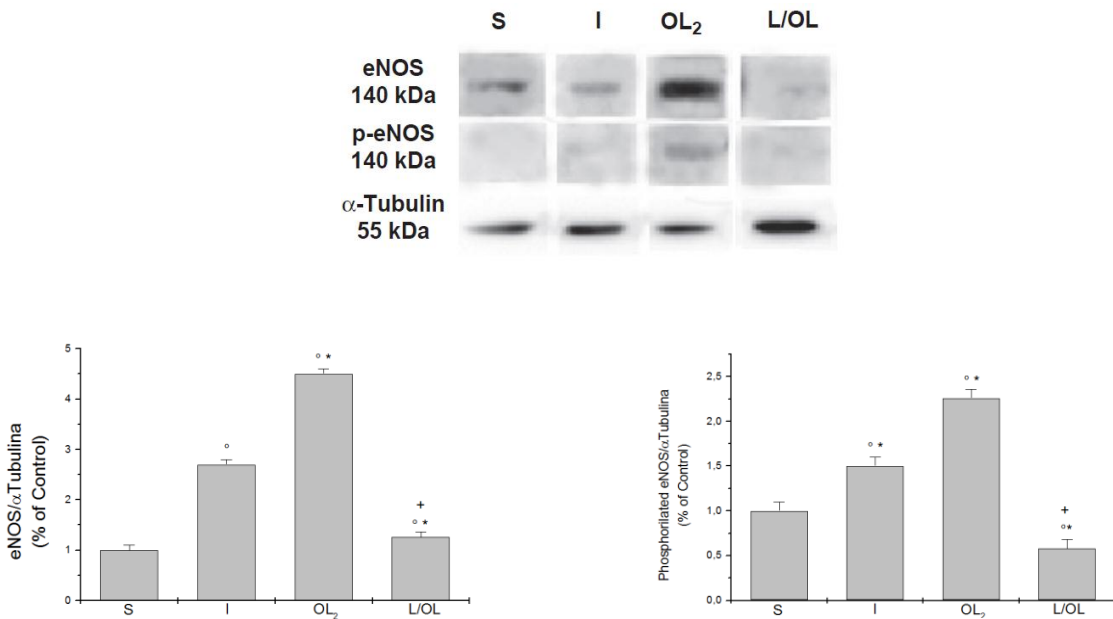


Fig. 4.1.2.: Western blotting of eNOS expression and phosphorilated eNOS expression in two cerebral zones, cortex and striatum, at RE in S = sham operated subgroup; I = hypoperfused group; OL<sub>2</sub> = oleuropein subgroup (20 mg/kg b.w.); L/OL = L-NIO (10 mg/kg b.w.) and oleuropein (20 mg/kg b.w.) group; <sup>o</sup>p < 0.01 vs. S subgroup and baseline, \*p < 0.01 vs. I group, +p < 0.01 vs. OL<sub>2</sub> subgroup

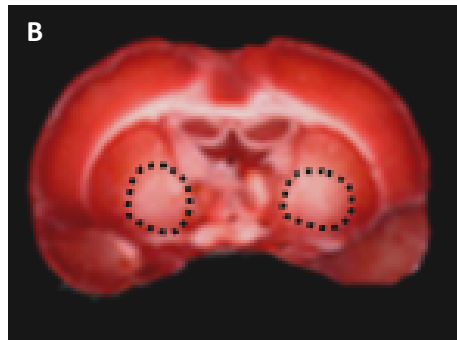
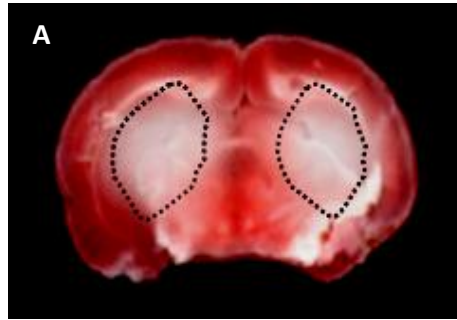


Fig. 4.1.3.: TTC staining of coronal brain slice from a rat submitted to BCCAO and reperfusion. The lesion in the striatum is outlined by the dashed black line (A). TTC staining of coronal brain slices from a rat treated with higher dose oleuropein (20 mg/kg b.w.) (B).

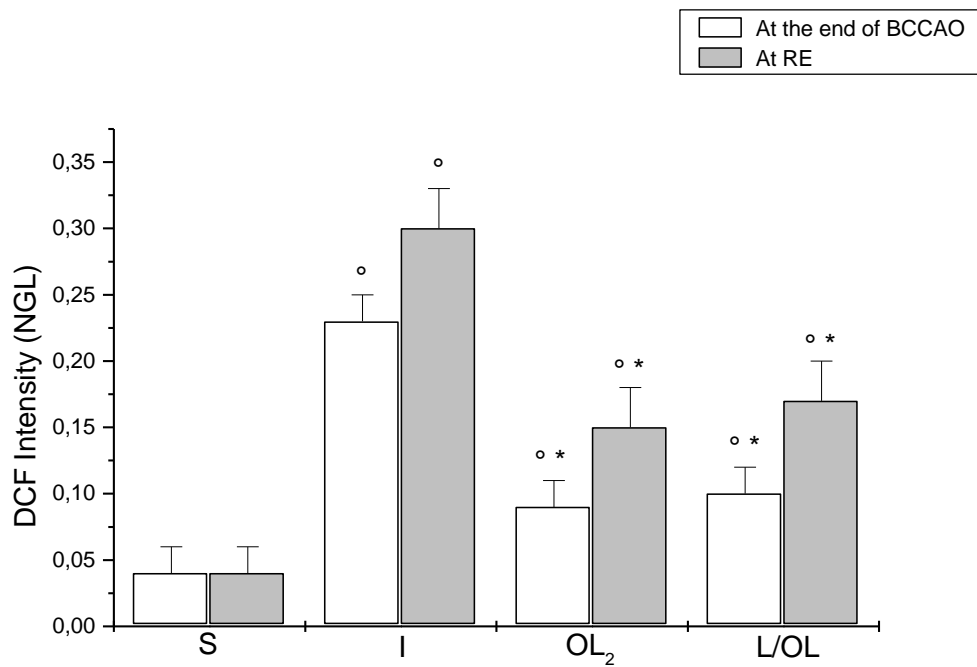


Fig. 4.1.4.: Changes in DCF fluorescence intensity correlated to the intracellular ROS levels at the end of BCCAO and reperfusion (RE) in the different experimental groups: S = sham operated subgroup; I = hypoperfused group; OL<sub>2</sub>= oleuropein subgroup (20 mg/kg b.w.); L/OL = L-NIO (10 mg/kg b.w.) and oleuropein (20 mg/kg b.w.) group;

°p < 0.01 vs. S subgroup and baseline, \*p < 0.01 vs. I group.

## **4.2 The clinical study**

### **4.2.1 Nutritional status evaluation**

Under baseline conditions, all obese patients showed significant differences in anthropometric measurements compared to normal weight ones. In particular, patients belonging to O and HO groups had a significant higher waist circumference, indicating an increased cardiovascular risk for these women (Table 4.2). Moreover, hyperlipidemic females showed an altered lipid profile, with higher total cholesterol, LDL cholesterol and triglycerides levels, compared to obese and normal weight controls (Table 4.2).

After three months of hypocaloric and hypolipidic diet all obese patients showed a significant reduction in BMI and anthropometric parameters, as well as an improvement in body composition (Tables 4.2.1.).

Furthermore, after three months dieting, a significant decrease in total serum cholesterol, LDL cholesterol and triglycerides was detected in OD and OL groups (Table 4.2.2). However, the reduction in total and LDL cholesterol appeared higher in patients treated with oleuropein, compared to hyperlipidemic controls (Table 4.2.2). After three months, indeed, Total and LDL cholesterol reduced by  $15.0 \pm 1.2$  % and  $16.5 \pm 1.3$  % in OD group, treated with the only diet, and by  $21.3 \pm 1.5$  % and  $21.2 \pm 1.4$  % in OL group, treated with diet plus oleuropein (Fig.4.2, 4.2.1). Moreover, we did not observed significant changes in serum GOT and GPT in all groups (data not shown).

### **4.2.2 SBF evaluation under resting conditions**

Under baseline conditions, laser Doppler signals revealed significant differences between normal weight, obese and hyperlipidemic obese patients. HO and O groups showed lower perfusion values compared to normal weight one even though the skin blood flow of hyperlipidemic patients was lower compared to obese subjects ( $8.0 \pm 0.5$  vs  $9.1 \pm 0.6$  vs  $12.0 \pm 0.5$  PU;  $p < 0.01$  vs O and NW groups; Fig.4.2.2). Moreover, the spectral analysis revealed that total PSD was lower in obese and hyperlipidemic females compared to normal weight ones ( $65.0 \pm 4.1$  vs  $127.3 \pm 6.0$  vs  $200.5 \pm 5.5$  PU<sup>2</sup>/Hz;  $p < 0.01$  vs O and NW groups; Fig.4.2.3). The wavelet analysis was applied to all Laser Doppler signals revealing six frequency components in the range between 0.005 and 2 Hz, as previously reported [96]. Under baseline conditions, the power spectral density of neurogenic and myogenic activities appeared higher than those related to other parameters, however, the myogenic activity, expressed as percent of the total power spectral density, appeared significantly lower in hyperlipidemic obese females compared to obese and normal weight patients ( $25.4 \pm 1.5$  vs  $30.8 \pm 2.0$  and  $36.0 \pm 2.6$  %,  $p < 0.01$  vs O and NW groups; Fig.4.2.4). On the other hand, the frequency component related to the respiration was higher in HO group, compared to normolipidemic obese and normalweight controls ( $12.5 \pm 1.3$  vs  $10.2 \pm 1.1$  vs  $9.8 \pm 0.9$  %,  $p < 0.01$  vs O and NW groups).

### **4.2.3 SBF evaluation after three months dieting**

After three months of hypocaloric and hypolipidic diet all hyperlipidemic obese patients showed a significant improvement in SBF (Fig.4.2.5) and total PSD of LDPM oscillations. In particular, SBF increased by  $25.6 \pm 1.4$  % of baseline in patients administered with oleuropein plus dieting, while the increase appeared lower in OD group ( $+12.5 \pm 1.2$  %,  $p < 0.01$  vs  $T_0$ ). Moreover, total PSD of LDPM signals significantly increased in both groups even though we did not detect significant differences between OD and OL groups.

Furthermore, the spectral analysis of skin blood flow oscillations revealed significant changes compared to baseline conditions. After weight reduction OD as well as OL groups showed a significant increase in the myogenic related component, compared to baseline values ( $29.7 \pm 2.5$  vs  $25.4 \pm 1.5$  % and  $35.8 \pm 3.2$  vs  $24.6 \pm 1.5$ ,  $p < 0.01$  vs  $T_0$ ; Fig. 4.2.6, 4.2.7). Interestingly, OL group showed higher percentage increase in the myogenic-related frequency component, compared to OD one (Fig.4.2.7). This change in the total power spectrum was accompanied by a significant decrease in the respiratory-related frequency component and a significant increase in NO-dependent frequency component, compared to baseline conditions (Fig.4.2.7.).

#### **4.2.4 PORH evaluation**

Under baseline conditions, the hyperemic response was significantly lower in HO and O groups, compared to NW one: in particular, we detected differences in all studied parameters, such as PK(max), Tp and PK (%) (Table 4.2.3). Moreover, the peak value was lower in hyperlipidemic obese subjects than in normolipidemic ones ( $31.1 \pm 2.8$  vs  $37.3 \pm 2.6$  and  $59.1 \pm 2.3$  PU, respectively;  $p < 0.01$  vs O and NW groups) as well as the percent increase from baseline ( $402.9 \pm 3.8$  vs  $528.8 \pm 6.4$  and  $769.9 \pm 8.0$  %, respectively;  $p < 0.01$  vs O and NW groups), and the time to peak ( $12.5 \pm 0.6$  vs  $9.1 \pm 0.7$  and  $7.0 \pm 0.8$  seconds, respectively;  $p < 0.01$  vs O and NW group; Table 4.2.3.).

After three months of dietary treatment a significant improvement in hyperemic response was detected in all obese subjects, compared to baseline conditions. In particular, OD and OL groups showed a significant increase in peak value ( $46.5 \pm 3.1$  vs  $29.9 \pm 2.4$  and  $65.2 \pm 2.3$  vs  $32.3 \pm 2.8$  PU, respectively,  $p < 0.01$  vs  $T_0$ ; Fig. 4.2.8.) and in total percent increase from baseline ( $616.3 \pm 4.6$  vs  $405.5 \pm 3.0$  and  $749.1 \pm 4.0$  vs  $402.2 \pm 4.7$ %, respectively;  $p < 0.01$  vs  $T_0$ ; Fig. 4.2.9.); on the other hand the time to peak significantly reduced, compared to baseline conditions ( $7.4 \pm 0.5$  vs  $12.7 \pm 0.4$  and  $9.3 \pm 0.6$  vs  $12.3 \pm 0.8$  seconds, in OD and OL groups respectively;  $p < 0.01$  vs  $T_0$ ; Figure 4.2.10).

	<b>NW GROUP (n=20)</b>	<b>O GROUP (n=20)</b>	<b>HO GROUP (n=40)</b>
	T <sub>0</sub>	T <sub>0</sub>	T <sub>0</sub>
<b>BMI (kg/m<sup>2</sup>)</b>	23.5±1.2	34.8±1.1*	35.0±0.5*
<b>WC (cm)</b>	84.1±1.3	105.7±1.6*	105.1±1.2*
<b>HC (cm)</b>	97.4±1.4	113.8±2.0*	113.0±1.8*
<b>TS (mm)</b>	17.5±1.3	31.3±1.6*	31.4±1.4*
<b>FM (%)</b>	31.6±1.3	41.5±1.3*	39.9±1.1*
<b>FFM (%)</b>	68.4±1.5	58.7±1.9*	59.7±1.4*
<b>Total cholesterol (mg/dL)</b>	184.6±3.6	191.2±1.5	255.7±3.7* <sup>o</sup>
<b>HDL cholesterol (mg/dL)</b>	60.6±2.4	58.6±2.8	52.2±2.5
<b>LDL cholesterol (mg/dL)</b>	113.7±2.4	122.6±2.3	173.7±4.3* <sup>o</sup>
<b>Triglycerides (mg/dL)</b>	130.5±4.1	132.1±3.5	180.2±4.1* <sup>o</sup>

Table 4.2.: Anthropometric measurements [body mass index (BMI), waist circumference (WC), hip circumference (HF) and triceps skinfold (TS)], body composition [Fat Mass (FM) and Fat Free Mass (FFM)] and metabolic parameters [Total cholesterol, HDL cholesterol, LDL cholesterol and triglycerides] under baseline conditions (T<sub>0</sub>) in normalweight (NW), normolipidemic obese (O group) and hyperlipidemic obese (HO group) patients.

Data are reported as mean ± SEM.

\*p<0.01 vs NW group; <sup>o</sup>p<0.01 vs O group.

	OD GROUP		OL GROUP	
	T <sub>0</sub>	T <sub>1</sub>	T <sub>0</sub>	T <sub>1</sub>
<b>BMI (kg/m<sup>2</sup>)</b>	36.2±0.4	31.9±0.6*	34.2±0.5	31.7±0.4 *
<b>WC (cm)</b>	104.9±1.4	99.2±1.1*	105.4±1.3	98.9±1.2*
<b>HC (cm)</b>	112.6±1.8	109.8±2.2°	113.5±1.6	111.0±1.7
<b>TS (mm)</b>	29.8±1.3	26.8±1.2*	33.0±1.5	31.4±1.5*
<b>FM (%)</b>	42.2±1.3	39.9±1.4*	37.6±0.9	35.5±1.3*
<b>FFM (%)</b>	57.0±1.9	58.3±1.9	62.4±0.9	64.5±1.3*

Table 4.2.1.: Anthropometric measurements [body mass index (BMI), waist circumference (WC), hip circumference (HF) and triceps skinfold (TS)], body composition [Fat Mass (FM) and Fat Free Mass (FFM)] and metabolic parameters [Total cholesterol, HDL cholesterol, LDL cholesterol and triglycerides under baseline conditions (T<sub>0</sub>) and after three months dieting in oleuropein-treated group (OL) and hyperlipidemic controls (OD).

Data are reported as mean ± SEM.

\*p<0.01 vs T<sub>0</sub>; °p<0.05 vs T<sub>0</sub>

	OD GROUP			OL GROUP		
	T <sub>0</sub>	T <sub>1</sub>	Δ	T <sub>0</sub>	T <sub>1</sub>	Δ
<b>Total cholesterol (mg/dL)</b>	255.0±3.4	216.9±3.6*	-38.1	256.5±3.2	202.0±3.3* <sup>+</sup>	-54.5
<b>HDL cholesterol (mg/dL)</b>	56.6±2.0	51.4±2.4	-5.2	47.8±3.0	44.2±3.1	-3.6
<b>LDL cholesterol (mg/dL)</b>	168.4±3.5	140.6±2.4*	-27.8	179.0±4.2	141.2±2.5* <sup>+</sup>	-37.8
<b>Triglycerides (mg/dL)</b>	193.8±4.3	156.2±4.0*	-37.6	166.7±4.5	126.4±3.8*	-40.3

Table 4.2.2.: Total cholesterol, HDL cholesterol, LDL cholesterol and triglycerides under baseline conditions (T<sub>0</sub>) and after three months dieting (T<sub>1</sub>) in oleuropein-treated group (OL) and hyperlipidemic controls (OD).

Data are reported as mean ± SEM.

\*p<0.01 vs T<sub>0</sub>; °p<0.05 vs T<sub>0</sub>; +p<0.01 vs OD (T<sub>0</sub>)

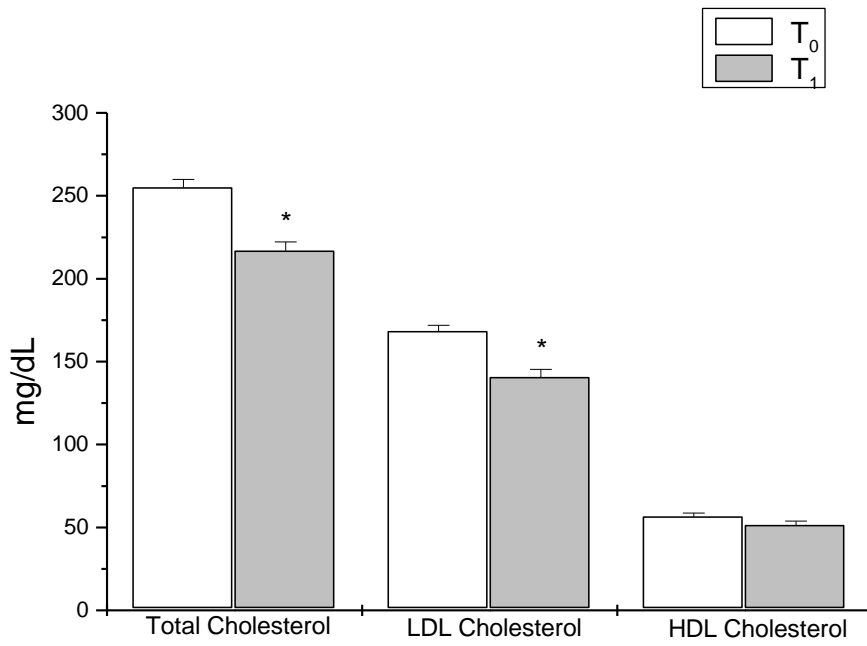


Fig. 4.2.: Total cholesterol, LDL cholesterol and HDL cholesterol under baseline conditions (T<sub>0</sub>) and after three months of hypocaloric and hypolipidic diet in OD group.

\*p<0.01 vs T<sub>0</sub>.

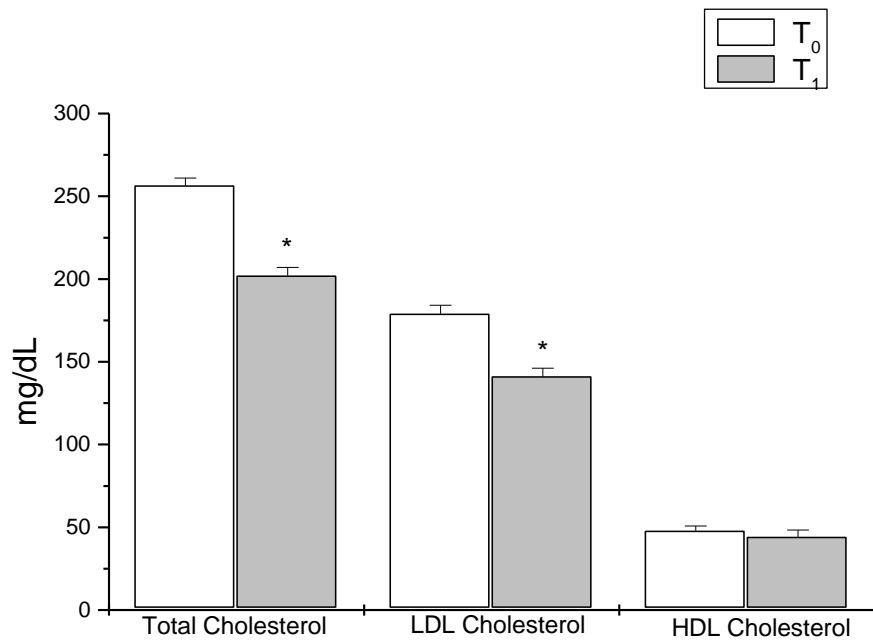


Fig. 4.2.1.: Total cholesterol, LDL cholesterol and HDL cholesterol under baseline conditions (T<sub>0</sub>) and after three months of hypocaloric and hypolipidic diet plus oleuropein in OL group.

\*p<0.01 vs T<sub>0</sub>.

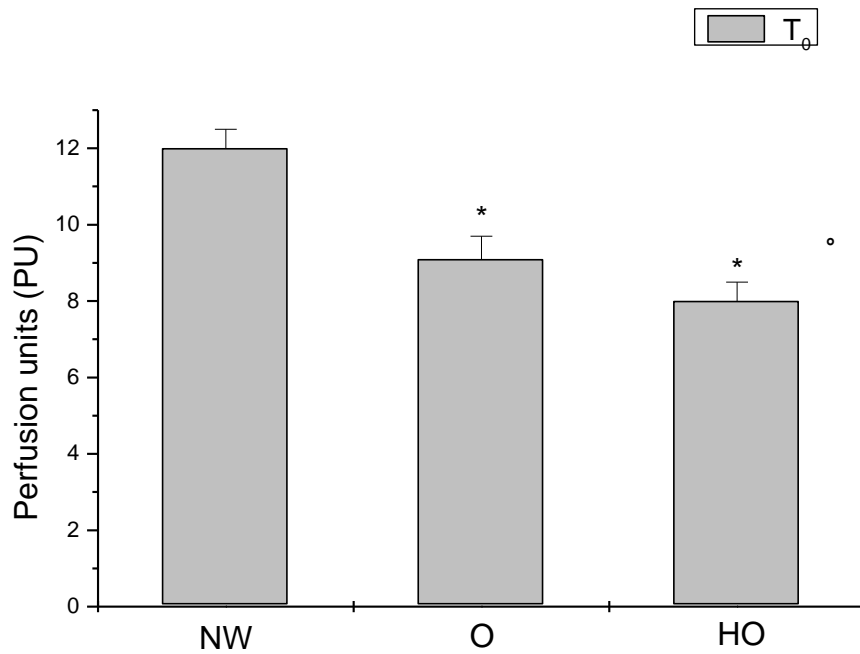


Fig.4.2.2.: Skin microvascular blood flow, expressed as Perfusion Units (PU), under baseline conditions ( $T_0$ ) in normal weight (NW group), normolipidemic obese (O group) and hyperlipidemic obese subjects (HO group).

\* $p < 0.01$  vs NW group;

° $p < 0.01$  vs O group.

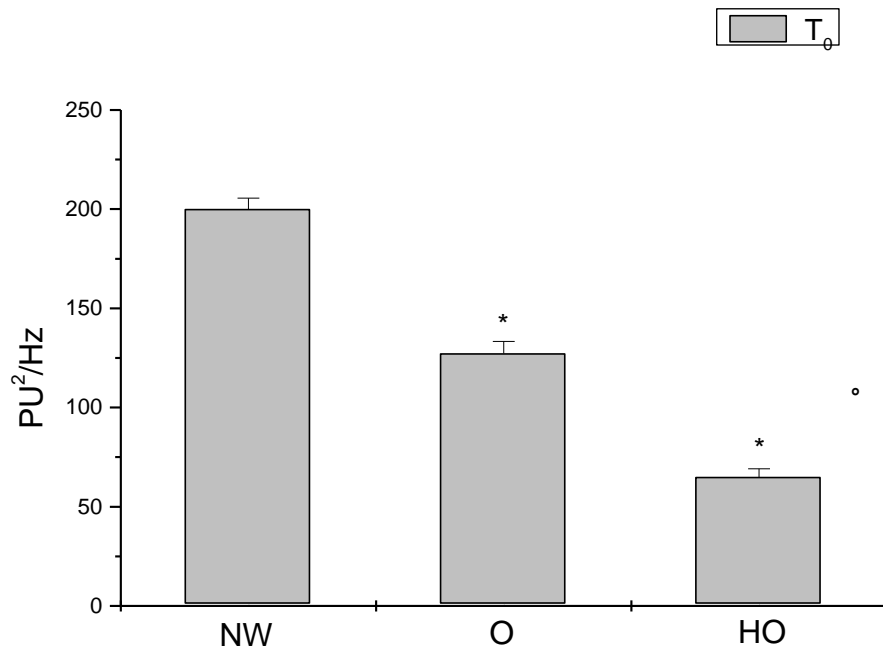


Fig.4.2.3.: Total Power Spectral Density, expressed as  $PU^2/Hz$ , under baseline conditions ( $T_0$ ) in normalweight (NW group), normolipidemic obese (O group) and hyperlipidemic obese subjects (HO group).

\* $p < 0.01$  vs NW group, ° $p < 0.01$  vs O group

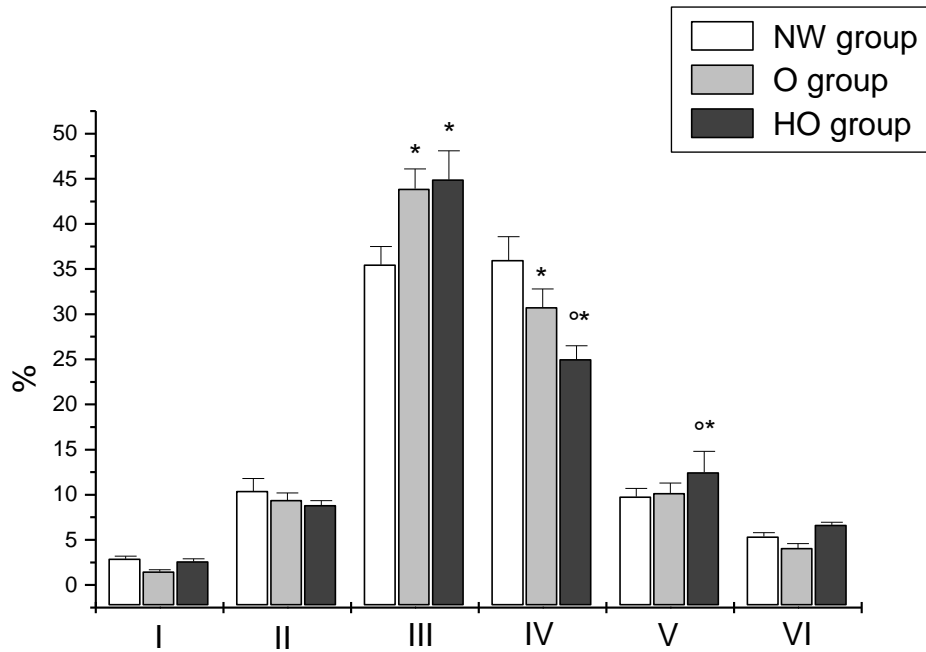


Fig.4.2.4.: Normalized power spectral density, expressed as percent, related to NO-independent endothelial activity (1), NO-dependent endothelial activity (2), neurogenic activity (3), myogenic activity (4), respiration (5) and heart rate (6) under baseline conditions ( $T_0$ ) in normal weight (NW), normolipidemic obese (O) and hyperlipidemic obese patients (HO).

\*  $p < 0.01$  vs  $T_0$  NW group, °  $p < 0.01$  vs  $T_0$  O group.

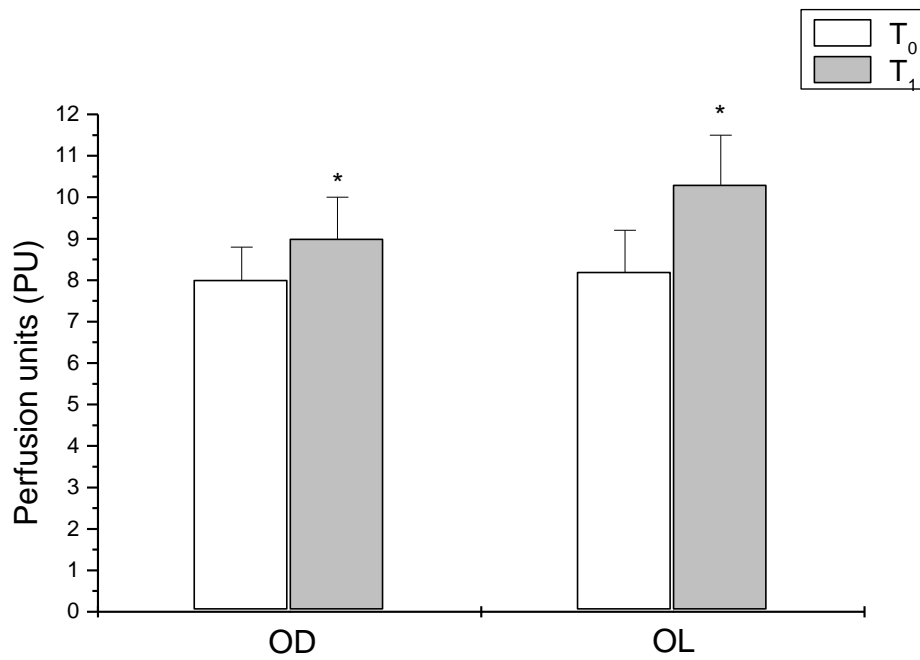


Fig.4.2.5.: Skin microvascular blood flow, expressed as Perfusion Units (PU), under baseline conditions (T<sub>0</sub>) and after three months of hypocaloric and hypolipidic diet (T<sub>1</sub>), in hyperlipidemic obese controls (OD group) and oleuropein-treated group (OL group).

\*p<0.01 vs T<sub>0</sub>

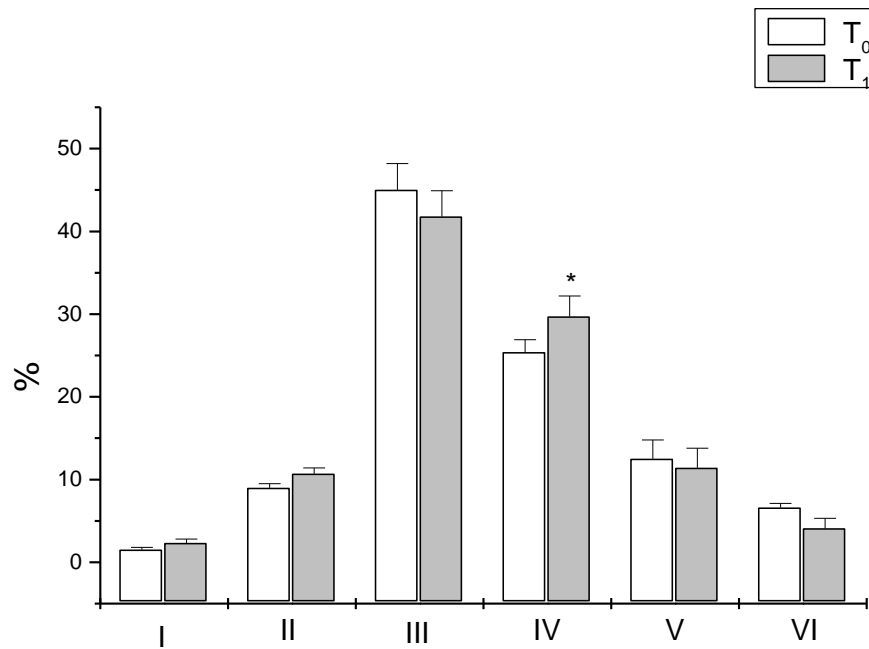


Fig.4.2.6.: Normalized power spectral density, expressed as percent, related to NO-independent endothelial activity (1), NO-dependent endothelial activity (2), neurogenic activity (3), myogenic activity (4), respiration (5) and heart rate (6) under baseline conditions (T<sub>0</sub>) and after three months of hypocaloric and hypolipidic diet in hyperlipidemic obese controls (OD group).

\* p < 0.01 vs T<sub>0</sub>

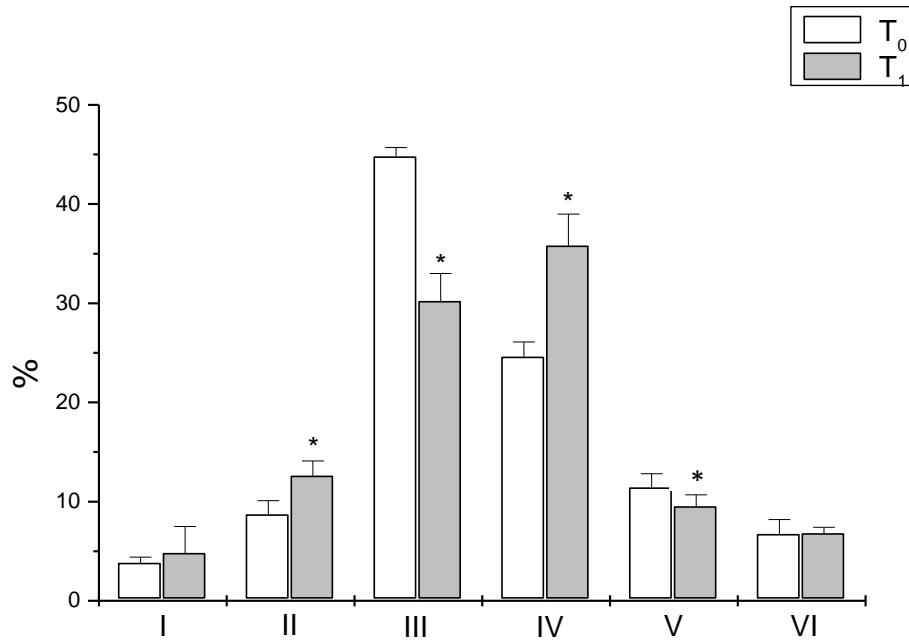


Fig.4.2.7.: Normalized power spectral density, expressed as percent, related to NO-independent endothelial activity (1), NO-dependent endothelial activity (2), neurogenic activity (3), myogenic activity (4), respiration (5) and heart rate (6) under baseline conditions (T<sub>0</sub>) and after three months of hypocaloric and hypolipidic diet (T<sub>1</sub>) in oleuropein-treated group (OL group).

\* p < 0.01 vs T<sub>0</sub>

Groups	PK (PU)	PORH (%)	Tp (sec)	Duration of hyperemia (sec)
NW	59.1±2.3	767.2±8.0	7.0±0.8	49.2±2.9
O	37.3±2.6*	525.5±6.4*	9.1±0.7°	41.5±3.4°
HO	31.1±2.8*+	402.2±3.8*+	12.5±0.6*+	37.1±3.1*

Table 4.2.3: Post-occlusive reactive hyperemia (PORH) peak (PK), expressed as perfusion units (PU); PORH total increase, expressed as percent (%); time to peak (Tp), expressed as seconds (sec); duration of hyperemia (sec), under baseline conditions in NW, O and HO groups.

\* p< 0.01 vs T<sub>0</sub> NW group; °p<0.05 vs T<sub>0</sub> NW group; +p<0.01 vs T<sub>0</sub> O group

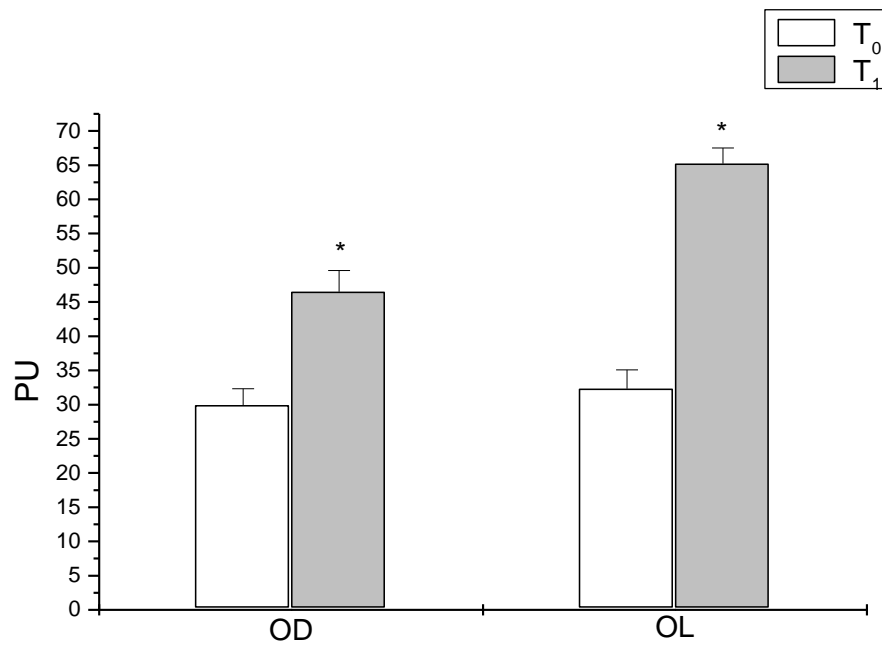


Fig.4.2.8.: Post-occlusive reactive hyperemia peak, expressed as perfusion units (PU), under baseline conditions (T<sub>0</sub>) and after three months of hypocaloric and hypolipidic diet (T<sub>1</sub>) in OD and OL groups.

\*p<0.01 vs T<sub>0</sub>.

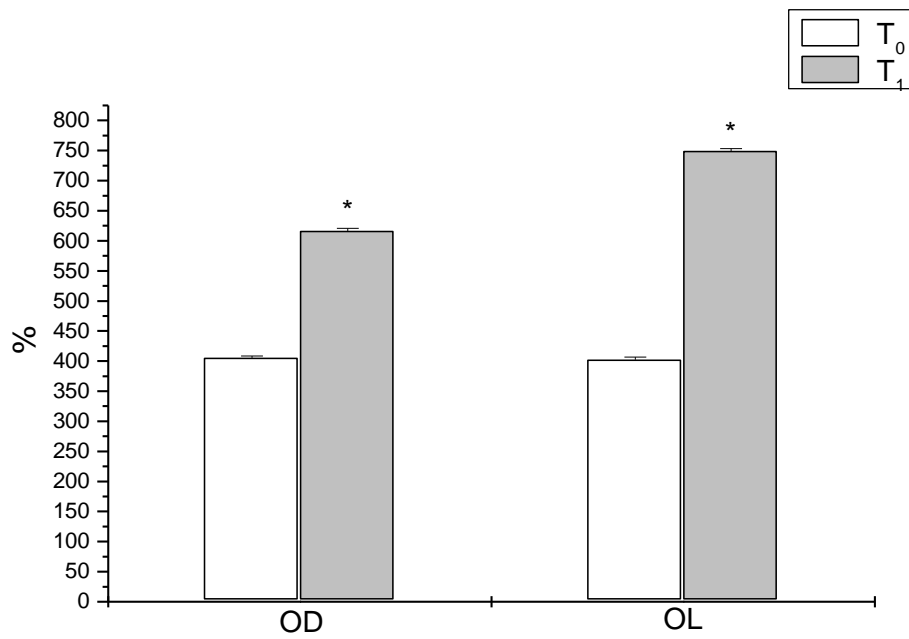


Fig.4.2.9.: Percent increase in post-occlusive reactive hyperemia, under baseline conditions (T<sub>0</sub>) and after three months of hypocaloric and hypolipidic diet (T<sub>1</sub>) in OD and OL groups.

\*p<0.01 vs T<sub>0</sub>.

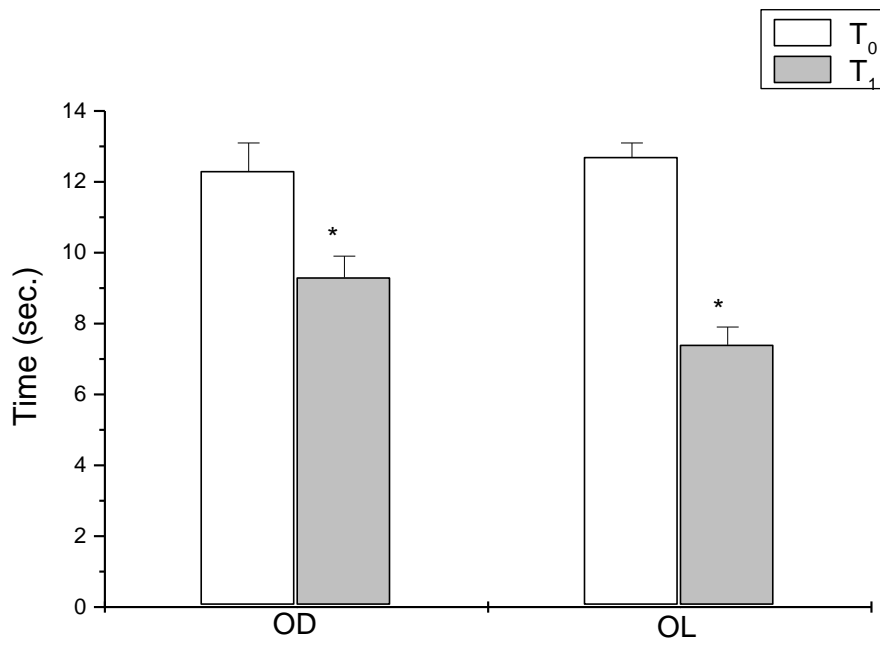


Fig4.2.10.: Time to peak, expressed in seconds, under baseline conditions (T<sub>0</sub>) and after three months of hypocaloric and hypolipidic diet (T<sub>1</sub>) in OD and OL groups.

\* p < 0.01 vs T<sub>0</sub>

## Chapter 5

### Discussion

The results of the present study indicate that oleuropein was able to improve microvascular functions in rats and humans. It is well known, indeed, that 30 min of hypoperfusion and 60 min of reperfusion in rat brain induce significant microvascular alterations, characterized by a decrease in arteriolar diameter, increase in microvascular leakage, leukocyte adhesion to venules and reduction in capillary perfusion, as previously reported [122]. The *in vivo* study allowed us to visualize the pial arteriolar tree characterizing the microvascular networks on the brain surface, where the arterioles are involved in the vascular resistance regulation, according to their geometric features. The significant reduction in diameter, observed in order 3 arterioles at the end of reperfusion, in hypoperfused rats, was accompanied by an increase in microvascular leakage, indicated by FD70 extravasation from vessels to the interstitium, and by leukocyte adhesion to venular wall. These alterations are representative of the blood brain barrier damage and tissue perfusion reduction.

Interestingly, oleuropein, a polyphenol widely diffused in olive plants derivatives, protected rat pial microcirculation after BCCAO and reperfusion. Previous studies indicate that oleuropein shows several anti-oxidant and anti-inflammatory properties. This molecule is able, indeed, to reduce LDL oxidation and plasmatic cholesterol levels in rabbits as well as to protect isolated rat hearts from ischemia-reperfusion injury, reducing creatine kinase production and the reduced glutathione release [41,42]. Moreover, oleuropein appears able to inhibit the biosynthesis of several pro-inflammatory cytokines, such as tumor necrosis factor  $\alpha$  (TNF- $\alpha$ ) and interleukin-1 beta (IL-1 $\beta$ ) [43].

In our study, at the end of BCCAO, 20 mg/kg b.w. oleuropein abolished the decrease in diameter in all arteriolar orders and prevented microvascular leakage, compared to hypoperfused animals. LDF measurements confirmed these data indicating that pial blood flow appeared higher in treated animals, compared to hypoperfused controls. At the end of reperfusion, oleuropein higher dosage induced a strong arteriolar vasodilation increasing the blood flow by  $28 \pm 2\%$  of baseline. These vasodilatory effects were abolished by L-

NIO, a specific eNOS inhibitor, administered prior to oleuropein, indicating that this polyphenol could induce e-NOS expression and NO release from endothelial cells. Furthermore, oleuropein acute administration reduced leukocyte adhesion to venules, at the end of reperfusion, decreasing the inflammatory response. Rats treated with oleuropein showed higher eNOS expressions, both total and phosphorylated proteins, in the cerebral cortex as well as in the striatum, indicating that this compound was able to enhance NO release. Moreover, oleuropein prevented oxidative stress reducing the ischemic damage and protecting capillary perfusion.

To investigate oleuropein effects on human microcirculation, we measured the skin blood perfusion levels in hyperlipidemic obese patients by LDF. It is well known, indeed, that obesity and hyperlipidemia induce changes in microvascular function long before the formation of fatty streak lesions in large arteries [113,114]. In particular, LDF is a non-invasive technique allowing us to detect real-time changes in skin microvascular perfusion levels under baseline conditions as well as after acute stimuli, such as brachial artery occlusion. We chose to analyze cutaneous microcirculation because the skin is an easily accessible organ and its microvascular alterations can reflect the changes in other vascular beds, such as the cardiac one [123,124].

Interestingly, Stefanovska and coworkers demonstrated that skin blood flow oscillations can be analyzed by spectral methods to receive informations about the different local and central mechanisms regulating blood flow. Spectral analysis of LDF signals, indeed, reveals six different frequency intervals in the range between 0.005–2.0 Hz. These oscillations have been related to the influence of NO-independent and NO-dependent endothelial activities, sympathetic nervous system discharge, intrinsic myogenic activity of vascular smooth muscle cells, respiration and heart rate, as previously reported [94-96].

Under baseline conditions, all obese patients showed lower perfusion values, compared to normalweight ones, even though the skin blood flow appeared particularly low in hyperlipidemic subjects. These results confirm that obesity and hyperlipidemia affect arteriolar tone and tissue perfusion [101,102, 117-119]. In our study, the application of spectral analysis to LDF

signals showed that the power spectral density of frequency components related to neurogenic and myogenic activities were the predominant components of the total power spectrum, in all subjects. These data indicate that sympathetic nervous system discharge and the activity of smooth muscle cells were mainly involved in the regulation of microvascular blood flow distribution. However, normolipidemic obese subjects, as well as hyperlipidemic ones, were characterized by a significant decrease in the myogenic-related frequency component, compared to normalweight patients. These data are in accord with previous data, suggesting that obesity impairs smooth muscle cell tone. Interestingly, the activity of smooth muscle cells appeared lower in hyperlipidemic obese subjects, compared to normolipidemic obese controls. Therefore, it is possible to hypothesize that hyperlipidemia, associated to obesity, further affects smooth muscle cells activity increasing arteriolar stiffness in these patients. We detected also an increased respiratory-related frequency component in hyperlipidemic obese group, compared to controls, probably due to an increase in respiratory central drive on the microvascular blood flow.

Microvascular functions were further investigated evaluating the post-occlusive reactive hyperemia (PORH) in all patients. All obese females showed a reduced hyperemic response, compared to normalweight group, while hyperlipidemic subjects showed lower values. Therefore, our results indicate that obesity and hyperlipidemia altered microvascular function under baseline conditions as well as after acute stimulation, reducing the dilatory reserve of arterial vessels.

After three months dieting, all hyperlipidemic obese patients showed improvements in anthropometric measurements and body composition. Moreover, serum lipid profile of hyperlipidemic patients significantly improved, compared to baseline conditions. Interestingly, total and LDL cholesterol decreased by  $21.3 \pm 1.5$  and  $21.2 \pm 1.4\%$  of baseline in oleuropein-treated group and by  $15.0 \pm 1.2$  and  $16.5 \pm 1.3\%$  of baseline in hyperlipidemic controls. These results are in accord with several *in vivo* studies suggesting that oleuropein is able to improve lipid profile [41]. These changes in nutritional status and lipid profile were accompanied by an improvement in perfusion

values and skin blood flow oscillations, after three months treatment. We detected, indeed, significant changes in the total power spectral density of both groups patients. In particular, evaluating the frequency components of blood flow oscillations, the myogenic-related frequency component significantly increased in both groups, even though the increase was higher in oleuropein-treated group, compared to controls. Furthermore, the high frequency component related to respiration significantly decreased, while the spectral density of the NO-dependent frequency component significantly increased in oleuropein-treated group. These results indicate that the amplitude of blood flow oscillations increased after oleuropein administration, due to the improvement in endothelial and myogenic activities. At the same time, there was a reduction in the respiratory central drive influence on peripheral blood flow. These effects may indicate a higher activity of vascular endothelial and smooth muscle cells.

Moreover, these patients showed an improvement in hyperemic response, suggesting a recovery in endothelial and smooth muscle cell functions. However, it is important to point out that reactive hyperemia results from the interplay of several regulatory mechanisms, such as metabolic and endothelial vasodilators, the myogenic response and sympathetic nervous system discharge. Among endothelial vasodilators, NO, EDHF and prostaglandins, particularly prostacyclin, are mainly implicated in human skin hyperemic response [133,134]. Therefore, the evaluation of reactive hyperemia by LDF represents an useful non-invasive tool in evaluating the global microvascular function [135].

We know there are several non-invasive methods to investigate vascular function. Among these, the evaluation of flow mediated dilation (FMD) by ultrasound has been widely used in the clinical research to investigate endothelial dysfunction under several pathological conditions. This method, introduced in 1992, allow one to measure brachial artery diameter changes after ischemic stimulation. The acute stimulation induces nitric oxide release from endothelium determining a vasodilation that can be assessed and visualized by ultrasound imaging. The brachial artery is observed above the antecubital fossa in the longitudinal plane. In particular, a segment with clear

anterior and posterior intimal interfaces between the lumen and vessel wall is selected for continuous 2D grayscale imaging, as previously reported. FMD has been widely used in the clinical practice demonstrating the presence of endothelial dysfunction in many pathological conditions, such as diabetes and hypertension. It is worth noting that the reproducibility of reactive hyperemia by LDF is similar to that of brachial artery by flow-mediated dilation, as previously reported [136,137]. Moreover, many studies report a significant correlation between FMD and LDF measurements. However, variations in arteries smaller than 2.5 mm in diameter are difficult to measure by FMD [136]. Therefore, cutaneous LDF may represent a simple, non-invasive tool to assess microvascular function in the daily practice.

In the present study, we focused our attention on skin microcirculation because these peripheral arteriolar networks are mainly involved in the regulation of blood flow distribution. Several studies investigated the flowmotion by LDF under different pathological conditions, such as hypertension, diabetes and hypercholesterolemia indicating an impaired flow-dependent vasodilation [61,62]. Moreover, the application of spectral analysis to the skin blood flow oscillations reveals that three months dieting plus oleuropein improved the activity of smooth muscle cells and NO release from endothelial cells.

In conclusion, oleuropein appears able to improve microvascular function in rats increasing NO release from endothelial cells, reducing ROS production and facilitating tissue perfusion. Moreover, this polyphenol, associated to dieting, appears able to improve serum lipid profile and tissue perfusion in hyperlipidemic obese females.

## References

1. Sofi F., Cesari F., Abbate R., Gensini G.F., Casini A. Adherence to Mediterranean diet and health status: meta-analysis. *BMJ* 2008; 337
2. Sofi F., Abbate R., Gensini G.F., Casini A. Accruing evidence on benefits of adherence to the Mediterranean diet on health: an updated systematic review and meta-analysis. *Am J Clin Nutr* 2010;92:1189–96
3. Panagiotakos DB, Pitsavos C, Stefanadis C. Dietary patterns: a Mediterranean diet score and its relation to clinical and biological markers of cardiovascular disease risk. *Nutr Metab Cardiovasc Dis.* 2006 Dec;16(8):559-68.
4. Scarmeas N, Stern Y, Tang MX, Mayeux R, Luchsinger JA. Mediterranean diet and risk for Alzheimer's disease. *Ann Neurol.* 2006 Jun;59(6):912-21.
5. Lukas Schwingshackl, Georg Hoffmann. Monounsaturated fatty acids, olive oil and health status: a systematic review and meta-analysis of cohort studies. *Lipids Health Dis.* 2014; 13: 154.
6. Bulotta S, Celano M, Lepore SM, Montalcini T, Pujia A, Russo D. Beneficial effects of the olive oil phenolic components oleuropein and hydroxytyrosol: focus on protection against cardiovascular and metabolic diseases. *J Transl Med.* 2014 Aug 3;12:219.
7. Peyrol J, Riva C, Amiot M. Hydroxytyrosol in the Prevention of the Metabolic Syndrome and Related Disorders. *Nutrients.* 2017 Mar 20;9(3).
8. Sarbishegi M, Mehraein F, Soleimani M. Antioxidant role of oleuropein on midbrain and dopaminergic neurons of substantia nigra in aged rats. *Iran Biomed J.* 2014;18(1):16-22.
9. Schabauer AM, Rooke TW. Cutaneous laser Doppler flowmetry: applications and findings. *Mayo Clin Proc.* 1994 Jun;69(6):564-74.
10. Kvandal P, Stefanovska A, Veber M, Kvernmo HD, Kirkebøen KA. Regulation of human cutaneous circulation evaluated by laser Doppler flowmetry, iontophoresis, and spectral analysis: importance of nitric oxide and prostaglandines. *Microvasc Res.* 2003 May;65(3):160-71
11. Keys A, Menotti A, Karvonen MJ, et al. The diet and 15-year death rate in the Seven Countries Study. *Am J Epidemiol* 1986; 124: 903-15.

12. Mancini M, Stamler J. Diet for preventing cardiovascular diseases: Light from Ancel Keys, distinguished centenarian scientist. *NMCD - Nutritional, Metabolism and Cardiovascular Diseases* 2004; 14: 52-7.
13. The Mediterranean diet. UNESCO Nomination file 2010-n.00394 , punto D, p. 4.
14. Verschuren WMM, Jacobs DR, et al. Serum total cholesterol and long-term coronary heart disease mortality in different cultures. Twenty-five year follow-up of the Seven Countries Study. *JAMA* 1995; 274: 131-6.
15. Hoffman R., Gerber M. *The Mediterranean Diet: Health and Science*, Wiley- Blackwell, 2013
16. Trichopoulou A, Bamia C, Trichopoulos D. Anatomy of health effects of Mediterranean diet: Greek EPIC prospective cohort study. *BMJ*. 2009
17. Martínez-González MA, Salas-Salvadó J, Estruch R, Corella D, Fitó M, Ros E; PREDIMED INVESTIGATORS. Benefits of the Mediterranean Diet: Insights From the PREDIMED Study. *Prog Cardiovasc Dis*. 2015; 58(1):50-60.
18. Guasch-Ferré M, Hu FB, Martínez-González MA, Fitó M, Bulló M, Estruch R, Ros E, Corella D, Recondo J, Gómez-Gracia E et al. Olive oil intake and risk of cardiovascular disease and mortality in the PREDIMED Study. *BMC Med*. 2014 May 13;12:78.
19. Boskou D. Olive Oil Quality in Boskou D. (Ed.) *Olive Oil: Chemistry and Technology*. AOCS Press, Champaign, IL, USA, 1996, 101-120
20. Cultivars
21. Emekli-Alturfan E., Kasikci E., Yarat A. Effects of oleic acid on the tissue factor activity, blood lipids, antioxidant and oxidant parameters of streptozotocin induced diabetic rats fed a high-cholesterol diet. *Medicinal Chemistry Research* 2010, Volume 19, Issue 8, pp 1011–1024
22. Ghanbari R, Anwar F, Alkharfy KM, Gilani AH, Saari N. Valuable nutrients and functional bioactives in different parts of olive (*Olea europaea* L.)-a review. *Int J Mol Sci*. 2012;13(3):3291-340.
23. Shahidi F., Ambigaipalan P. Phenolics and polyphenolics in foods, beverages and spices: Antioxidant activity and health effects – A review. *Journal of Functional Foods*, Volume 18, Part B, 2015, Pages 820-897.

24. Servili, M., Montedoro, G. (2002): Contribution of phenolic compounds of virgin olive oil quality, *Eur. J. Lipid Sci. Technol.* 104, 602- 613.
25. Montedoro G., Servili M., Baldioli M., Selvaggini M., Miniati E., Macchioni A. Simple and hydrolyzable compounds in virgin olive oil. 3. Spectroscopic characterizations of the secoiridoid derivatives. *J. Agric. Food Chem.*, 1993, 41 (11), pp 2228–223
26. Montedoro GF., Servili M., Baldioli M., Selvaggini R., Begliomini A.L., Taticchi A. Relationships between phenolic composition of olive fruit and olive oil: the importance of the endogenous enzymes. *Acta Horticulturae* (2001).
27. Gariboldi P., Jommi G., Verotta L. Secoiridoids from *Olea europaea*. *Phytochemistry* 25 (1986) 865-869.
28. Bourquelot E., Vintilesco J. C. R. Sur l'oleuropein, nouveau principe de nature glucosidique retré de l'olivier (*Olea europaea* L.). *Compt. Rend. Hebd. Acad. Sci., Paris (France)* 147 (1908) 533-535.
29. Panizzi L., Scarpati M.L., Oriente G. Chemical structure of oleuropein, bitter glucoside of olive with hypotensive activity. *Gazz. Chim. Ital.* 90 (1960) 1449-1485.
30. Ragazzi E., Veronese G., Guitto A. The demethyloleuropein, a new glucoside extracted from ripe olives. *Ann.Chim.* 63 (1973) 13-20.
31. Oliveras-López MJ, Berná G, Carneiro EM, López-García de la Serrana H, Martín F, López MC. An extra-virgin olive oil rich in polyphenolic compounds has antioxidant effects in OF1 mice. *J Nutr.* 2008 Jun;138(6):1074-8.
32. Fernández-Castillejo S, Valls RM, Castañer O, Rubió L, Catalán Ú, Pedret A, Macià A, Sampson ML, Covas MI, Fitó M, Motilva MJ, Remaley AT, Solà R1. Polyphenol rich olive oils improve lipoprotein particle atherogenic ratios and subclasses profile: A randomized, crossover, controlled trial. *Mol Nutr Food Res.* 2016 Jul;60(7):1544-54.
33. Tuck KL1, Hayball PJ. Major phenolic compounds in olive oil: metabolism and health effects. *J Nutr Biochem.* 2002 Nov;13(11):636-644.
34. Briante R, Patumi M, Terenziani S, Bismuto E, Febbraio F, Nucci R. *Olea europaea* L. leaf extract and derivatives: antioxidant properties. *J Agric Food Chem.* 2002 Aug 14;50(17):4934-40.

35. Soler-Rivas C, Espin JC, Wichers HJ. Oleuropein and related compounds. *J Sci Food Agric.* 2000;80:1013–1023.
36. Amiot MJ, Fleuriet A, Macheix JJ. Importance and evolution of phenolic compounds in olive during growth and maturation. *J Agric Food Chem.* 1986;34:823–826.
37. Amiot MJ, Fleuriet A, Macheix JJ. Accumulation of oleuropein derivatives during olive maturation. *Phytochemistry.* 1989;28:67–70.
38. Limiroli R, Consonni R, Ottolina G, Marsilio V, Bianchi G, Zetta L. <sup>1</sup>H and <sup>13</sup>C NMR characterization of new oleuropein aglycones. *J Chem Soc Perkin Trans 1.* 1995:1519–1523.
39. Visioli F, Bellomo G, Galli C. Free radical-scavenging properties of olive oil polyphenols. *Biochem Biophys Res Commun.* 1998 Jun 9;247(1):60-4.
40. Visioli F, Bellosta S, Galli C. Oleuropein, the bitter principle of olives, enhances nitric oxide production by mouse macrophages. *Life Sci.* 1998;62(6):541-6.
41. Coni E, Di Benedetto R, Di Pasquale M, Masella R, Modesti D, Mattei R, Carlini EA. Protective effect of oleuropein, an olive oil biophenol, on low density lipoprotein oxidizability in rabbits. *Lipids.* 2000 Jan;35(1):45-54.
42. Manna C, Migliardi V, Golino P, Scognamiglio A, Galletti P, Chiariello M, Zappia V. Oleuropein prevents oxidative myocardial injury induced by ischemia and reperfusion. *J Nutr Biochem.* 2004 Aug;15(8):461-6.
43. Impellizzeri D., Esposito E., Mazzon E., Paterniti I., di Paola R., Bramanti P., Morittu V.M., Procopio A., Britti D., Cuzzocrea S. The effects of oleuropein aglycone, an olive oil compound, in a mouse model of carrageenan-induced pleurisy. *Clin. Nutr.* 2011;30:533–540.
44. Jemai H, Fki I, Bouaziz M, Bouallagui Z, El Feki A, Isoda H, Sayadi S. Lipid-lowering and antioxidant effects of hydroxytyrosol and its triacetylated derivative recovered from olive tree leaves in cholesterol-fed rats. *J Agric Food Chem.* 2008;56:2630–2636.
45. M.N. Vissers, P.L. Zock, A.J.C. Roodenburg, R. Leenen, M.B. Katan Olive oil phenols are absorbed in humans. *J. Nutr.*, 132 (2002), pp. 409-417
46. de Bock M, Derraik JG, Brennan CM, Biggs JB, Morgan PE, Hodgkinson SC, Hofman PL, Cutfield WS. Olive (*Olea europaea* L.) leaf polyphenols

- improve insulin sensitivity in middle-aged overweight men: a randomized, placebo-controlled, crossover trial. *PLoS One*. 2013;8(3):e57622.
47. Omar SH. Oleuropein in Olive and its Pharmacological Effects. *Sci Pharm*. 2010 Apr-Jun; 78(2): 133–154.
  48. Ronald F. Tuma, Walter N. Duran, Klaus Ley. *Microcirculation*. Elsevier, 2011
  49. Di Sarah Y. Yuan, Robert R. Rigor. *Regulation of Endothelial Barrier Function*. Morgan and Claypool life sciences, 2010
  50. Jones T.W. Discovery that the veins of the bat's wing are endowed with rhythmical contractility and that onward flow of blood is accelerated by each contraction. *Philos. Trans. Roy. Soc. Lond*. 1852;142:131–136.
  51. Colantuoni A, Bertuglia S, Intaglietta M. Quantitation of rhythmic diameter changes in arterial microcirculation. *Am J Physiol* 1984; 246: H508-17.
  52. Fagrell B, Intaglietta M, Ostergren J. Relative hematocrit in human skin capillaries and its relationship to capillary flow velocity. *Microvasc Res* 1980; 20: 327-35.
  53. Salerud GE, Tenland T, Nilsson GE, Oberg AP. Rhythmical variations in human skin microcirculation. *Int J Microcirc Clin Exp* 1983; 2: 91-102.
  54. Kaufman AG, Intaglietta M. Automated diameter measurement of vasomotion by cross-correlation. *Int J Microcirc Clin Exp* 1985; 4, 45–53.
  55. Mahler F, Muheim MH, Intaglietta M, Bollinger A, Anliker M. Blood pressure fluctuations in human nailfold capillaries. *Am J Physiol* 1979; 236, H888–H893.
  56. Aalkjær C., Nilsson H. Vasomotion: cellular background for the oscillator and for the synchronization of smooth muscle cells. *Br J Pharmacol*. 2005 Mar; 144(5): 605–616.
  57. Jackson, W.F., Mulsch, A. & Busse, R. 1991. Rhythmic smooth muscle activity in hamster aortas is mediated by continuous release of NO from the endothelium. *Am J Physiol* 260, H248–H253.
  58. Gustafsson, H., Mulvany, M.J. & Nilsson, H. 1993. Rhythmic contractions of isolated small arteries from rat: influence of the endothelium. *Acta Physiol Scand* 148, 153–163.

59. Ursino M, Colantuoni A, Bertuglia S. Vasomotion and blood flow regulation in hamster skeletal muscle microcirculation: A theoretical and experimental study. *Microvasc Res.* 1998 Nov;56(3):233-52.
60. Mauban JR, Wier WG. Essential role of EDHF in the initiation and maintenance of adrenergic vasomotion in rat mesenteric arteries. *Am J Physiol Heart Circ Physiol.* 2004 Aug;287(2):H608-16.
61. Rossi, M., Carpi, A., Di, M.C., Galetta, F. & Santoro, G. Spectral analysis of laser-Doppler skin blood flow oscillations in human essential arterial hypertension. *Microvasc Res.* 2006a.72, 34–41.
62. Bouskela, E. Effects of metformin on the wing microcirculation of normal and diabetic bats. *Diabete Metab* 1988. 14, 560–565.
63. Stansberry, K.B., Shapiro, S.A., Hill, M.A., McNitt, P.M., Meyer, M.D. & Vinik, A.I. Impaired peripheral vasomotion in diabetes. *Diabetes Care* 1996.19, 715–721.
64. Hill MA, Zou H, Potocnik SJ, Meininger GA, Davis MJ. Invited review: arteriolar smooth muscle mechanotransduction: Ca(2+) signaling pathways underlying myogenic reactivity. *J Appl Physiol* (1985). 2001 Aug;91(2):973-83.
65. Uchida E and Bohr DF. Myogenic tone in isolated perfused resistance vessels from rats. *Am J Physiol* 216: 1343–1350, 1969.
66. Davis MJ, Meininger GA, and Zawejja DC. Stretch-induced increases in intracellular calcium of isolated vascular smooth muscle cells. *Am J Physiol Heart Circ Physiol* 263: H1292– H1299, 1992.
67. Hamill OP and Martinac B. Molecular basis of mechanotransduction in living cells. *Physiol Rev* 81: 685–740, 2001.
68. Kirber MT, Guerrero-Hernandez A, Bowman DS, Fogarty KE, Tuft RA, Singer JJ, and Fay FS. Multiple pathways responsible for the stretch-induced increase in Ca<sup>2+</sup> concentration in toad stomach smooth muscle cells. *J Physiol (Lond)* 524: 3–17, 2000.
69. Kirber MT, Walsh JV, and Singer JJ. Stretch-activated ion channels in smooth muscle: a mechanism for the initiation of stretch-induced contraction. *Pflugers Arch* 412: 339–345, 1988.
70. Conti et al. *Fisiologia medica*. Volume 2. Edi-ermes. 2010.

71. Boron W.F., Boulpaep E. L. *Medical Physiology*. Elsevier Health Sciences, 2008
72. Balligand J.L., Feron O., Dessy C. eNOS Activation by Physical Forces: From Short-Term Regulation of Contraction to Chronic Remodeling of Cardiovascular Tissues. *Physiol Rev* 89: 481–534, 2009
73. Förstermann U, Münzel T. Endothelial nitric oxide synthase in vascular disease: from marvel to menace. *Circulation*. 2006 Apr 4;113(13):1708-14.
74. Kaufman AG, Intaglietta M. Automated diameter measurement of vasomotion by cross-correlation. *Int J Microcirc Clin Exp* 1985; 4, 45–53.
75. Forbes HS. The cerebral circulation: observation and measurement of pial vessels. *Arch Neurol Psychiatry* 19:751-761, 1928
76. Rosenblum WI, Zweifach BW (1963) Cerebral microcirculation in the mouse brain. *Arch Neurol* 9:414-423
77. Wahl M, Deetjen P, Thurau K, Ingvar DH, Lassen NA. Micropuncture evaluation of the importance of perivascular pH for the arteriolar diameter on the brain surface. *Pflügers. Arch* 316:152-163, 1970
78. Navari RM, Wei EP, Kontos HA, Patterson JL (1978) Comparison of the open skull and cranial window preparations in the study of the cerebral microcirculation. *Microvasc Res*16:304-315
79. Morii S, Ngai AC, Winn HR. Reactivity of rat pial arterioles and venules to adenosine and carbon dioxide: with detailed description of the closed cranial window technique in rats. *J Cereb Blood Flow Metab*. 1986 Feb;6(1):34-41.
80. Lapi D, Marchiafava PL, Colantuoni A. Geometric characteristics of arterial network of rat pial microcirculation. *J Vasc Res*. 2008;45(1):69-77. Epub 2007 Sep 27.
81. Bollinger A, Hoffmann U, Franzeck UK. Evaluation of flux motion in man by the laser-Doppler technique. *Blood Vessels* 1991; 28(Suppl. 1), 21–26.
82. Tsai AG, Intaglietta M. Evidence of flowmotion induced changes in local tissue oxygenation. *Int J Microcirc Clin Exp* 1993; 12, 75–88.
83. Oberg PA. Laser-Doppler flowmetry. *Critical Reviews in Biomedical Engineering*, 1990, 18(2):125-163
84. Saumet JL, Dittmar A, Leftheriotis G. Non-invasive measurement of skin blood flow: comparison between plethysmography, laser-Doppler

- flowmeter and heat thermal clearance method. *Int J Microcirc Clin Exp*. 1986;5(1):73-83.
85. Rossi M, Carpi A, Di Maria C, Galetta F, Santoro G. Spectral analysis of laser Doppler skin blood flow oscillations in human essential arterial hypertension. *Microvasc Res*. 2006 Jul-Sep;72(1-2):34-41. 2006
  86. Farkas K, Kolossváry E, Járαι Z, Nemcsik J, Farsang C. Non-invasive assessment of microvascular endothelial function by laser Doppler flowmetry in patients with essential hypertension. *Atherosclerosis*. 2004 Mar;173(1):97-102.
  87. Tur E, Yosipovitch G, Bar-On Y. Skin reactive hyperemia in diabetic patients. A study by laser Doppler flowmetry. *Diabetes Care*. 1991 Nov;14(11):958-62.
  88. Kruger A, Stewart J, Sahityani R, O'Riordan E, Thompson C, Adler S, Garrick R, Vallance P, Goligorsky MS. Laser Doppler flowmetry detection of endothelial dysfunction in end-stage renal disease patients: correlation with cardiovascular risk. *Kidney Int*. 2006 Jul;70(1):157-64. 2006
  89. Meyer JU, Borgstrom P, Lindblom L, Intaglietta M (1988) Vasomotion patterns in skeletal muscle arterioles during changes in arterial pressure. *Microvasc Res* 35:193–203
  90. Hoffman U, Franzeck UK, Geiger M, Bollinger A (1990) Variability of different patterns of skin oscillatory flux in healthy controls and patients with peripheral arterial occlusive disease. *Int J Microcirc Clin Exp* 12:255–273
  91. Morlet, J., 1983. Sampling theory and wave propagation. In: Chen, C.H. (Ed.), *Issues in Acoustic Signal/Image Processing and Recognition*. NATO ASI Series, vol. I. Springer-Verlag, pp. 233–261.
  92. Stefanovska A (1992) Self-organization of biological systems influenced by electrical current. Thesis, Faculty of Electrical Engineering, University of Ljubljana, Slovenia
  93. Muck-Weymann ME, Albrecht H-P, Hager D, Hiller D, Hornstein OP, Bauer RD (1996) Respiratory-dependent laser-Doppler flux motion in different skin areas and its meaning to autonomic nervous control of the vessels of the skin. *Microvasc Res* 52:69–78

94. Stefanovska A, Kroelj P. Correlation integral and frequency analysis of cardiovascular functions. *Open Systems and Information Dynamics* archive 1997; 4.
95. Kvandal P, Landsverk SA, Bernjak A, Stefanovska A, Kvernmo HD, Kirkebøen KA. Low-frequency oscillations of the laser doppler perfusion signal in human skin. *Microvascular Research* 2006; 72: 120–127.
96. Stefanovska A, Bracic M, Kvernmo HD. Wavelet analysis of oscillations in the peripheral blood circulation measured by laser Doppler technique. *IEEE Trans Biomed Eng* 1999; 46:1230–1239.
97. Rossi M, Maurizio S, Carpi A. Skin blood flowmotion response to insulin iontophoresis in normal subjects. *Microvasc Res* 2005; 70:17–22.
98. Rossi M, Santoro G, Ricco R, Pentimone F, Carpi A. Effect of chronic aerobic exercise on cutaneous microcirculatory flow response to insulin iontophoresis and to ischemia in elderly males. *Int J Sports Med* 2005; 26: 558–562.
99. GBD 2015 Obesity Collaborators. Health Effects of Overweight and Obesity in 195 Countries over 25 Years. *N Engl J Med*. 2017
100. OKkio alla SALUTE - EpiCentro - Istituto Superiore di Sanità, 2016
101. Kershaw EE, Flier JS. Adipose tissue as an endocrine organ. *J Clin Endocrinol Metab*. 2004 Jun;89(6):2548-56.
102. Shen W, Punyanitya M, Chen J, Gallagher D, Albu J, Pi-Sunyer X, Lewis CE, Grunfeld C, Heshka S, Heymsfield SB. Waist circumference correlates with metabolic syndrome indicators better than percentage fat. *Obesity (Silver Spring)*. 2006 Apr;14(4):727-36.
103. Gabriely I, Ma XH, Yang XM, Atzmon G, Rajala MW, Berg AH, Scherer P, Rossetti L, Barzilai N. Removal of visceral fat prevents insulin resistance and glucose intolerance of aging: an adipokine-mediated process? *Diabetes*. 2002 Oct;51(10):2951-8.
104. Jonk AM, Houben AJ, de Jongh RT, Serné EH, Schaper NC, Stehouwer CD. Microvascular dysfunction in obesity: a potential mechanism in the pathogenesis of obesity-associated insulin resistance and hypertension. *Physiology (Bethesda)*. 2007 Aug;22:252-60.
105. De Filippis E, Cusi K, Ocampo G, Berria R, Buck S, Consoli A, Mandarino LJ. Exercise-induced improvement in vasodilatory function

- accompanies increased insulin sensitivity in obesity and type 2 diabetes mellitus. *J Clin Endocrinol Metab* 91: 4903–4910, 2006.
106. de Jongh RT, Serne EH, RGIJ, de Vries G, Stehouwer CD. Impaired microvascular function in obesity: implications for obesity-associated microangiopathy, hypertension, and insulin resistance. *Circulation* 109: 2529–2535, 2004.
107. Steinberg HO, Chaker H, Leaming R, Johnson A, Brechtel G, Baron AD. Obesity/insulin resistance is associated with endothelial dysfunction. Implications for the syndrome of insulin resistance. *J Clin Invest* 97: 2601–2610, 1996.
108. Arcaro G, Zamboni M, Rossi L, Turcato E, Covi G, Armellini F, Bosello O, Lechi A. Body fat distribution predicts the degree of endothelial dysfunction in uncomplicated obesity. *Int J Obes Relat Metab Disord* 23: 936–942, 1999.
109. Clerk LH, Vincent MA, Jahn LA, Liu Z, Lindner JR, Barrett EJ. Obesity blunts insulin-mediated microvascular recruitment in human forearm muscle. *Diabetes* 55: 1436–1442, 2006.
110. Frisbee JC. Hypertension-independent microvascular rarefaction in the obese Zucker rat model of the metabolic syndrome. *Microcirculation* 12: 383–392, 2005.
111. Stepp DW. Impact of obesity and insulin resistance on vasomotor tone: nitric oxide and beyond. *Clin Exp Pharmacol Physiol* 33: 407–414, 2006.
112. Ross, R. Atherosclerosis: an inflammatory disease. *N. Engl. J. Med.* 340:115–126; 1999.
113. Scalia, R.; Appel, J. Z. III; Lefer, A. M. Leukocyte-endothelium interaction during the early stages of hypercholesterolemia in the rabbit: role of P-selectin, ICAM-1, and VCAM-1. *Arterioscler. Thromb. Vasc. Biol.* 18:1093–1100; 1998.
114. Stokes, K. Y.; Clanton, E. C.; Russell, J. M.; Ross, C. R.; Granger, D. N. NAD(P)H oxidase-derived superoxide mediates hypercholesterolemia-induced leukocyte-endothelial cell adhesion. *Circ. Res.* 88:499–505; 2001.
115. Tailor, A.; Granger, D. N. Acute hypercholesterolemia and ischemia/reperfusion-induced blood cell-endothelial cell adhesion in the murine mesenteric vascular bed. *FASEB J.* 15:A35; 2001

116. Takahashi, K.; Ohyanagi, M.; Ikeoka, K.; Iwasaki, T. Acetylcholine-induced response of coronary resistance arterioles in cholesterol-fed rabbits. *Jpn. J. Pharmacol.* 81:156–162; 1999.
117. Gilligan, D. M.; Guetta, V.; Panza, J. A.; Garcia, C. E.; Quyyumi, A. A.; Cannon, R. O. III Selective loss of microvascular endothelial function in human hypercholesterolemia. *Circulation* 90:35–41; 1994.
118. Napoli, C.; Lerman, L. O. Involvement of oxidation-sensitive mechanisms in the cardiovascular effects of hypercholesterolemia. *Mayo Clin. Proc.* 76:619–631; 2001.
119. Kohno, M.; Murakawa, K.; Yasunari, K.; Yokokawa, K.; Horio, T.; Kano, H.; Minami, M.; Yoshikawa, J. Improvement of erythrocyte deformability by cholesterol-lowering therapy with pravastatin in hypercholesterolemic patients. *Metabolism* 46:287–291; 1997.
120. Granger, D. N. Ischemia/reperfusion: mechanisms of microvascular dysfunction and the influence of risk factors for cardiovascular disease. *Microcirculation* 6:167–178; 1999.
121. Gauthier, T. W.; Scalia, R.; Murohara, T.; Guo, J. P.; Lefer, A. M. Nitric oxide protects against leukocyte-endothelium interactions in the early stages of hypercholesterolemia. *Arterioscler. Thromb. Vasc. Biol.* 15:1652–1659; 1995.
122. Lapi D, Vagnani S, Pignataro G, Esposito E, Paterni M, Colantuoni A. Protective effects of quercetin on rat pial microvascular changes during transient bilateral common carotid artery occlusion and reperfusion. *Front Physiol* 3: 1–12, 2013.
123. Jung F, Mrowietz C, Labarrere C: Primary cutaneous microangiopathy in heart recipients. *Microvasc Res* 62: 154-163, 2001.
124. Shamim-Uzzaman Q, Pfenninger D, Kehrer C: Altered cutaneous microvascular responses to reactive hyperemia in coronary artery disease: a comparative study with conduit vessel responses. *Clin Sci* 103: 267-273, 2002.
125. Rossi M, Carpi A, Di Maria C, Franzoni F, Galetta F, Santoro G. Skin blood flowmotion and microvascular reactivity investigation in hypercholesterolemic patients without clinically manifest arterial diseases. *Physiol Res.* 2009;58(1):39-47.

126. Ngai AC, Ko KR, Morii S, Winn HR. Effect of sciatic nerve stimulation on pial arterioles in rats. *Am J Physiol* 254: H133–H139, 1988.
127. Hudetz AG, Feher G, Weigle CGM, Knese DE, Kampine JP. Video microscopy of cerebrocortical capillary flow: response to hypotension and intracranial hypertension. *Am J Physiol* 268: H2202–H2210, 1985.
128. Bederson JB, Pitts H, Germano SM, Nishimura MC, Davis RL, Bartkowski HM. Evaluation of 2,3,5-triphenyltetrazolium chloride as a stain for detection and quantification of experimental cerebral infarction in rats. *Stroke* 17: 1304–1308, 1986.
129. Watanabe S. In vivo fluorometric measurement of cerebral oxidative stress using 2'-7'-dichlorofluorescein (DCF). *Keio J Med* 47: 92–98, 1998.
130. SINU. LARN - Livelli di assunzione di riferimento di nutrienti ed energia per la popolazione italiana - IV revisione, 2014.
131. Pala V, Sieri S, Palli D, Salvini S, Berrino F, Bellegotti M, Frasca G, Tumino R, Sacerdote C, Fiorini L, Celentano E, Galasso R, Krogh V. Diet in the Italian EPIC cohorts: presentation of data and methodological issues. *Tumori*. 2003;89(6):594–607.
132. Lee PH, Macfarlane DJ, Lam TH, Stewart SM. Validity of the International Physical Activity Questionnaire Short Form (IPAQ-SF): a systematic review. *Int J Behav Nutr Phys Act*. 2011;8:115.
133. Binggeli C, Spieker LE, Corti R, Sudano I, Stojanovic V, Hayoz D, Lüscher TF, Noll G. Statins enhance postischemic hyperemia in the skin circulation of hypercholesterolemic patients: a monitoring test of endothelial dysfunction for clinical practice? *J Am Coll Cardiol*. 2003 Jul 2;42(1):71-7.
134. Zhao JL, Pergola PE, Roman LJ, Kellogg DL Jr. Bioactive nitric oxide concentration does not increase during reactive hyperemia in human skin. *J Appl Physiol* (1985). 2004 Feb;96(2):628-32.
135. Cracowski JL, Minson CT, Salvat-Melis M, Halliwill JR. Methodological issues in the assessment of skin microvascular endothelial function in humans. *Trends Pharmacol Sci*. 2006 Sep;27(9):503-8. Epub 2006 Jul 31.
136. Corretti MC, Anderson TJ, Benjamin EJ, Celermajer D, Charbonneau F, Creager MA, Deanfield J, Drexler H, Gerhard-Herman M, Herrington D, Vallance P, Vita J, Vogel R; International Brachial Artery Reactivity Task

Force. Guidelines for the ultrasound assessment of endothelial-dependent flow-mediated vasodilation of the brachial artery: a report of the International Brachial Artery Reactivity Task Force. *J Am Coll Cardiol.* 2002 Jan 16;39(2):257-65.

137. Kubli S, Waeber B, Dalle-Ave A, Feihl F. Reproducibility of laser Doppler imaging of skin blood flow as a tool to assess endothelial function. *J Cardiovasc Pharmacol.* 2000 Nov;36(5):640-8.